Pharmaceutical Biology

ISSN: (Print) (Online) Journal homepage: informahealthcare.com/journals/iphb20

Molecular mechanisms underlying Tao-Hong-Si-Wu decoction treating hyperpigmentation based on network pharmacology, Mendelian randomization analysis, and experimental verification

Jun Chen & Wenyi Ye

To cite this article: Jun Chen & Wenyi Ye (2024) Molecular mechanisms underlying Tao-Hong-Si-Wu decoction treating hyperpigmentation based on network pharmacology, Mendelian randomization analysis, and experimental verification, Pharmaceutical Biology, 62:1, 296-313, DOI: 10.1080/13880209.2024.2330609

To link to this article: https://doi.org/10.1080/13880209.2024.2330609

PHARMACEUTICAL BIOLOGY
2024, VOL. 62, NO. 1, 296–313
https://doi.org/10.1080/13880209.2024.2330609

Taylor & Francis
Taylor & Francis Group

RESEARCH ARTICLE

Molecular mechanisms underlying Tao-Hong-Si-Wu decoction treating hyperpigmentation based on network pharmacology, Mendelian randomization analysis, and experimental verification

Jun Chen[a] and Wenyi Ye[b]

[a]Department of Geriatrics, The First Affiliated Hospital of Zhejiang Chinese Medical University (Zhejiang Provincial Hospital of Chinese Medicine), Hangzhou, China; [b]Department of Traditional Chinese Internal Medicine, The First Affiliated Hospital of Zhejiang Chinese Medical University (Zhejiang Provincial Hospital of Chinese Medicine), Hangzhou, China

ABSTRACT

Context: Hyperpigmentation, a common skin condition marked by excessive melanin production, currently has limited effective treatment options.

Objective: This study explores the effects of Tao-Hong-Si-Wu decoction (THSWD) on hyperpigmentation and to elucidate the underlying mechanisms.

Materials and methods: We employed network pharmacology, Mendelian randomization, and molecular docking to identify THSWD's hub targets and mechanisms against hyperpigmentation. The Cell Counting Kit-8 (CCK-8) assay determined suitable THSWD treatment concentrations for PIG1 cells. These cells were exposed to graded concentrations of THSWD-containing serum (2.5%, 5%, 10%, 15%, 20%, 30%, 40%, and 50%) and treated with α-MSH (100 nM) to induce an *in vitro* hyperpigmentation model. Assessments included melanin content, tyrosinase activity, and Western blotting.

Results: ALB, IL6, and MAPK3 emerged as primary targets, while quercetin, apigenin, and luteolin were the core active ingredients. The CCK-8 assay indicated that concentrations between 2.5% and 20% were suitable for PIG1 cells, with a 50% cytotoxicity concentration (CC_{50}) of 32.14%. THSWD treatment significantly reduced melanin content and tyrosinase activity in α-MSH-induced PIG1 cells, along with downregulating MC1R and MITF expression. THSWD increased ALB and p-MAPK3/MAPK3 levels and decreased IL6 expression in the model cells.

Discussion and conclusion: THSWD mitigates hyperpigmentation by targeting ALB, IL6, and MAPK3. This study paves the way for clinical applications of THSWD as a novel treatment for hyperpigmentation and offers new targeted therapeutic strategies.

ARTICLE HISTORY
Received 23 October 2023
Revised 26 February 2024
Accepted 2 March 2024

KEYWORDS
Tyrosinase; melanogenesis; inflammatory response

Introduction

Hyperpigmentation is a prevalent dermatologic condition, referring to the darkening of normal skin colour due to aberrantly high melanin or melanogenesis synthesis in skin melanocytes (Kumari et al. 2018; Giménez García and Carrasco Molina 2019). There are multiple causes of hyperpigmentation, such as inflammation, infection, pregnancy, hormonal factors, and aging (Xing et al. 2022). Post-inflammatory hyperpigmentation, melasma, solar lentigines, ephelides, and café au lait macules are representative hyperpigmentation conditions (Plensdorf et al. 2017). Hyperpigmentation can significantly affect self-esteem and quality of life, which has been one of the most universal reasons for patients of colour to seek dermatologic treatment (Wenner and Ramberg 2022). Hydroquinone-containing cream has been regarded as standard therapy for hyperpigmentation, and laser toning and chemical peels are alternative therapies (Yoo 2022). Unfortunately, these treatments have some deficiencies and adverse effects. It takes long time to show results, and patient compliance is poor (Nautiyal and Wairkar 2021). Therefore, more effective and safer therapeutic strategies for hyperpigmentation are required.

Traditional Chinese medicine (TCM) has long been applied to treat various diseases. Traditional Chinese herbs with skin whitening function, recorded in Ben-Cao-Gang-Mu, are widely used in China and have been shown to exert an anti-melanogenesis effect (Guo et al. 2021). For example, Atractylodis Rhizoma Alba extract inhibits melanin production by decreasing the expression of melanogenic enzymes (Chang et al. 2007). Furthermore, some TCM ingredients, such as salicylic acid (Liu et al. 2021) and mulberrosides (Liu et al. 2022), have exhibited their potential to mitigate hyperpigmentation disorders.

Tao-Hong Si-Wu decoction (THSWD) is a well-established TCM formula comprising *Persicae Semen*, *Carthami Flos*, *Angelicae Sinensis Radix*, *Paeoniae Radix Alba*, *Chuanxiong Rhizoma*, and *Rehmanniae Radix Praeparata* (Pan et al. 2022; Tang et al. 2022). Within this formula, *Persicae Semen* and *Carthami Flos* are recognized for their roles in facilitating blood

CONTACT Wenyi Ye yewenyi@zcmu.edu.cn Department of Traditional Chinese Internal Medicine, The First Affiliated Hospital of Zhejiang Chinese Medical University (Zhejiang Provincial Hospital of Chinese Medicine), No.54 Youdian Road, Hangzhou 310006, China

Supplemental data for this article can be accessed online at https://doi.org/10.1080/13880209.2024.2330609.

circulation and eliminating blood stasis. *Angelicae Sinensis Radix*, *Paeoniae Radix Alba*, *Chuanxiong Rhizoma*, and *Rehmanniae Radix Praeparata* are known to tonify *qi* and nourish blood according to the Chinese Pharmacopoeia (2020 edition). Recent pharmacological studies have highlighted the various activities of THSWD, including its anti-inflammatory (Wang et al. 2021), antioxidant (Xia et al. 2021), anti-tumour (Jiang et al. 2021), and anti-aging properties (Li et al. 2022). Given the emerging understanding of inflammation's role in melanogenesis, TCM treatments with strong anti-inflammatory effects, such as THSWD, are gaining attention as potential therapies for hyperpigmentation (Ding et al. 2020; Zhao et al. 2022; Luo et al. 2023). Studies have demonstrated the efficacy of THSWD in suppressing inflammation in skin scar tissues (Zhou et al. 2018; Zhang et al. 2023). Additionally, a recent study has shown that *Paeoniae Radix Alba*, a component of THSWD, can reduce pigmentation in synergy with four other TCM drugs (Guo et al. 2021). However, the specific effects of THSWD on hyperpigmentation have yet to be reported, indicating a significant area for future research.

Network pharmacology, an innovative approach, elucidates the molecular mechanisms of drugs treating various disorders through an interaction network that involves multiple genes, targets, and pathways (Li et al. 2022; Yang et al. 2022). This method has provided significant information and scientific reference for discovering TCM treatments (Zhu et al. 2022). In addition, Mendelian randomization (MR), a robust approach that uses single nucleotide polymorphisms (SNPs) as instrumental variables (IVs), has recently gained prominence. MR evaluates the causal relationships between exposure factors and outcomes (Khasawneh et al. 2022). Another key tool, molecular docking, widely used in drug discovery, estimates the binding structures of small molecule ligands to their appropriate target binding sites (Dong et al. 2018; Pinzi and Rastelli 2019).

This study uses network pharmacology to comprehensively explore the underlying mechanisms of THSWD against broadly defined hyperpigmentation rather than focusing on a specific form of this condition. MR analysis was conducted to identify the main therapeutic targets. Additionally, molecular docking and *in vitro* experiments were executed to verify the key targets and therapeutic effects of THSWD on hyperpigmentation. For the first time, this study uses integrated analyses to uncover the potential mechanisms through which THSWD treats hyperpigmentation, thus addressing a significant research gap in TCM drugs for this condition. The design and methodology of this study are illustrated in Figure 1.

Materials and methods

Screening of active ingredients of THSWD and related targets

To identify the active ingredients of THSWD, we utilized three primary databases: Herbal Ingredients' Targets (HIT; version 2.0, http://hit2.badd-cao.net) (Yan et al. 2022), Traditional Chinese Medicine Systems Pharmacology (TCMSP, http://tcmspw.com/tcmsp.php) (Ru et al. 2014), and Traditional Chinese Medicine Integrated Database (TCMID; version 2.0, http://www.megabionet.org/tcmid/) (Huang et al. 2018). The retrieved active ingredients were then normalized using the PubChem database (https://pubchem.ncbi.nlm.nih.gov/) (Kim et al. 2021). To ensure accuracy, duplicates were removed from the dataset.

Accurate assessment of absorption, distribution, metabolism, and excretion (ADME) properties is crucial in the discovery of effective drugs (Kumar et al. 2021). The quantitative estimate of drug-likeness (QED) method was applied to evaluate the ADME properties, setting the threshold at 0.2 (Bickerton et al. 2012; Yang et al. 2018). The targets for the active ingredients were identified using the HIT database, based on their PubChem IDs. Only targets corresponding to *Homo sapiens* species were selected. Active ingredients without target information were excluded. Standardization of target names was conducted using the UniProt database (https://www.uniprot.org/) (Lussi et al. 2023).

Screening of hyperpigmentation-related targets

Hyperpigmentation targets were retrieved from GeneCards (version 3.0; https://www.genecards.org/) (Safran et al. 2010) and DisGeNET (version 7.0, http://www.disgenet.org/) (Pinero et al. 2020) databases using the keyword 'hyperpigmentation'. The species was limited to *Homo sapiens*. The duplicate targets were eliminated, and the names were standardized using the UniProt database.

Acquisition of THSWD-hyperpigmentation overlapping targets

THSWD-associated and hyperpigmentation-associated targets were entered into VennDiagram (version 1.7.3, http://bioinfogp.cnb.csic.es/tools/venny/index.html) (Chen and Boutros 2011) to generate overlapping target set that was used for subsequent analyses. The THSWD-active ingredient-target network was constructed by running Cytoscape (version 3.7.1; https://cytoscape.org/download.html) (Legeay et al. 2020).

Gene ontology (GO) and Kyoto encyclopedia of genes and genomes (KEGG) pathway enrichment analyses

GO and KEGG pathway enrichment analyses were performed using the clusterProfiler package (version 4.4.2, https://bioconductor.org/packages/release/clusterProfiler.html) (Yu et al. 2012) with the species limited to *Homo sapiens*. GO analysis consisted of the biological process (BP), cellular component (CC), and molecular function (MF). The KEGG pathways were classified into six types: environmental information processing, human diseases, organismal systems, cellular processes, metabolism, and others. The following hypergeometric distribution model was used to determine whether the target gene set is significantly correlated with specific GO terms and pathways.

$$P = 1 - \sum_{i=0}^{k-1} \frac{\binom{M}{i}\binom{N-M}{N-i}}{\binom{N}{n}}$$

where n represents the total number of genes, m denotes the number of genes annotated in either GO or KEGG terms, n refers to the number of target genes, and k indicates the number of target genes. $p < 0.01$ indicates a significant GO or KEGG term (Yang et al. 2018).

Establishment of protein-protein interaction (PPI)

The PPI network was constructed by entering the THSWD hyperpigmentation overlapping targets into the Search Tool for the Retrieval of Interacting Genes/Proteins (STRING; https://string-db.org/) (Szklarczyk et al. 2021) and visualized using Cytoscape. The parameters of the applied PPI network were as

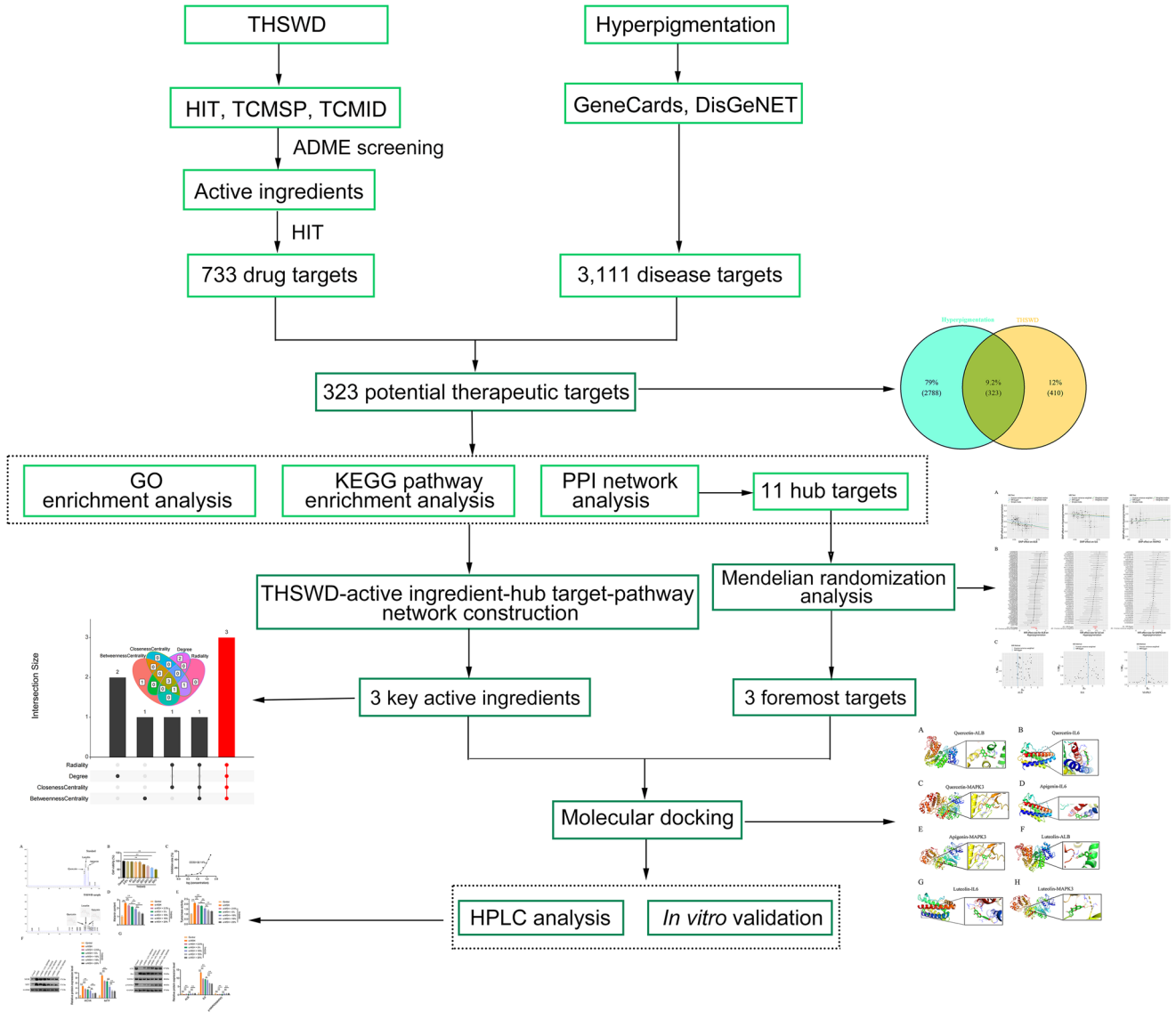

Figure 1. Workflow of the network pharmacology-based study, designed to investigate the anti-hyperpigmentation mechanisms of THSWD. THSWD, Tao-Hong-Si-Wu decoction.

follows: species, *Homo sapiens*; confidence score, more than 0.4; network type, full STRING network (default); size cut-off, no more than ten interactors (default). In addition, the top 20 hub targets were selected using the maximum neighborhood component (MNC), maximal clique centrality (MCC), and edge percolated component (EPC) algorithms of cytoHubba (version 0.1) (Chin et al. 2014), respectively. The above three algorithms effectively select hub genes from a PPI network (Chin et al. 2014). Intersecting the results of the three algorithms can enhance hub genes' reliability (Ma Z et al. 2021). The hub target networks were visualized using Cytoscape. The overlapping hub targets based on MNC, MCC, and EPC methods were identified using VennDiagram and used for molecular docking.

Construction of a THSWD-active ingredient-hub target-pathway network and screening of core active ingredients

The THSWD-active ingredient-hub target-pathway network was constructed using Cytoscape software. Common methods such as radiality, degree, closeness centrality, and betweenness centrality algorithms were employed to identify the hub nodes within this topological network (Chin et al. 2014). The top five active compounds were selected from the THSWD network using these four algorithms in Cytoscape. Subsequently, the UpSetR package (Conway et al. 2017) in the R software was used to intersect the top five active compounds identified by each method. This intersection approach was adopted to enhance the robustness of our findings. Active compounds consistently identified in all four methods were considered the most significant compounds of THSWD in treating hyperpigmentation.

MR analysis

Mendelian randomization is a causal inference method based on genetic variation. It uses genotypes as instrumental variables to reveal the causal relationship between a specific phenotype and a disease (Chen et al. 2022). As genetic variants are randomly distributed at conception, MR estimates are not influenced by confounding factors between exposure and outcome, reverse causation, or measurement errors (Carter et al. 2021). In this study, MR

analysis was conducted using the TwoSampleMR package (Lu et al. 2021) in R software (version 4.2.2). SNP data were sourced from the Genome-Wide Association Study (GWAS) database (https://gwas.mrcieu.ac.uk/) (Lyon et al. 2021). The inverse variance weighted (IVW) method was used to assess the causal relationship between key target genes and the risk of hyperpigmentation. Additionally, a sensitivity analysis was performed using the MR-Egger method (Burgess and Thompson 2017) to ensure the robustness of our findings. $p < 0.05$ indicates a significant causal link between a target gene and hyperpigmentation.

Molecular docking

Molecular docking was conducted to elucidate the interactions between specific hub target proteins and key active compounds. Crystal structures of these hub target proteins were obtained from the RCSB Protein Data Bank (PDB) (http://www.pdb.org/) (Goodsell et al. 2020). Using PyMOL and AutoDock (version 1.5.6), several preparatory steps were performed, including the removal of water molecules, isolation of the original ligand from the receptor, hydrogenation, repair of broken chains, and calculation of protein charge (Seeliger and de Groot 2010). The structures of the core active compounds were retrieved from ZINC (https://zinc.docking.org/) (Huang et al. 2021) and saved in the MOL2 format. Subsequently, Open Babel GUI software was used to convert all structural files into PDBQT format. The molecular docking process was then carried out using AutoDock1.5.6, and the results were analysed using PyMOL. Generally, a binding energy < −5.0 kcal/mol indicates a sound docking affinity, while a binding energy < −7.0 kcal/mol suggests a strong docking affinity (Feng et al. 2021). Docking pairs that met both criteria of having a binding energy of < − 5.0 kcal/mol and forming hydrogen bonds were considered to exhibit effective docking and were selected for further analysis.

High-performance liquid chromatography (HPLC) analysis

THSWD was purchased from Beijing Tongrentang, China, and its composition included 15 g of *Persicae Semen*, 15 g of *Carthami Flos*, 10 g of *Angelicae Sinensis Radix*, 10 g of *Paeoniae Radix Alba*, 10 g of *Chuanxiong Rhizoma*, and 10 g *Rehmanniae Radix Praeparata*. For analysis, 1.2169 g of THSWD powder was accurately weighed and then mixed with 50 mL of 90% ethanol (#10009218, Sinopharm, Beijing, China). This mixture underwent a 30-min ultrasound treatment and was subsequently cooled. The resulting supernatant was filtered through a 0.45-μm filter membrane for HPLC analysis. For the standard solution preparation, three control substances, quercetin (#B20527, Shanghai Yuanye Bio-Technology, China), apigenin (#B20981, Shanghai Yuanye Bio-Technology), and luteolin (#B20888, Shanghai Yuanye Bio-Technology), were precisely weighed and dissolved in methanol. This process yielded three concentrations of standard working solution (135.4 μg/mL, 137.8 μg/mL, and 138.5 μg/mL), which were also filtered through a 0.45-μm filter membrane. Quercetin (HPLC ≥ 98%; #B20527), apigenin (HPLC ≥ 98%; #B20981), and luteolin (HPLC ≥ 98%; #B20888) were supplied by Shanghai Yuanye, China.

HPLC analysis was performed on the 1260 Infinity II liquid chromatograph system (Angilent, Palo Alto, California, USA). A ChromCore C18-AC chromatographic column (5 μm, 4.6 mm × 250 mm; S009-050018-04625S, NanoChrom, Suzhou, China) was applied. The mobile phase consisted of methanol (A, #400642691, Sinopharm, Beijing, China) and 0.1% phosphoric acid (B, #2111201, Xilong Scientific, Shenzhen, China). The gradient elution procedure is shown in Table 1. The flow rate was set at 0.3 mL/min, the column temperature was 30 °C, and the detection wavelength was 270 nm, with an injection volume of 5 μL.

Experimental animals and preparation of serum THSWD

Twenty pathogen-free male Sprague-Dawley (SD) rats, 8 weeks and weighing approximately 200 ± 20 g, were procured from the Experimental Animal Center of Xiamen University, Xiamen, China. These rats were housed in cages under controlled environmental conditions: a temperature maintained at 21-23 °C, a relative humidity of 44-55%, and a 12 h light/dark cycle. They had *ad libitum* access to food and water. Following a one-week acclimatization period, rats were randomly divided into two groups: a blank group ($n = 10$) and a THSWD-treated group ($n = 10$).

Rats in the THSWD-treated group received 6 mL/kg of THSWD solution orally by gavage every 12 h for three consecutive days. In contrast, rats in the blank group were administered an equivalent volume of normal saline following the same schedule. One hour after the last gavage treatment, blood samples were collected from the abdominal aorta. All rats were euthanized using a 150 mg/kg dose of pentobarbital administered intraperitoneally. The blood samples collected were centrifuged at 3000 rpm for 20 min at 4 °C to separate the serum. This serum was inactivated in a 56 °C water bath for 30 min and filtered through a 0.22-μm membrane to remove bacteria. Finally, the serum was stored at −80 °C for future analysis.

All animal experiments complied with the Guide for the Care and Use of Laboratory Animals and were approved by the Animal Ethics Committee of Xiamen University (XMULAC20230175-2).

Cell culture, cell counting kit-8 (CCK-8) assay, and treatments

A human normal melanocyte cell line, PIG1 cells (CVCL_S410), was purchased from Shanghai Tongwei Biotechnology Co., Ltd, China (#TW34898). PIG1 cells were cultured in Dulbecco's modified Eagle medium (DMEM, #C11885500BT, Gibco, NY, USA) containing 10% fetal bovine serum (FBS, #34080619, Ephraim, Xiamen, China) and 1% penicillin-streptomycin at 37 °C with 5% CO_2.

CCK-8 assay was used to investigate and determine the appropriate concentrations of THSWD treatment for subsequent assays. Briefly, PIG1 cells were seeded in 96-well plates at a density of 2,000 cells per well. The cells were then exposed to gradient concentrations of THSWD (2.5%, 5%, 10%, 15%, 20%, 30%, 40%, and 50%). Following a 24-h incubation at 37 °C with 5% CO_2, cells were treated with 10 μL of CCK-8 solution (#C0037, Beyotime, Shanghai, China) for 2 h. Subsequently, cell viability was evaluated using a microplate reader (DR-3518G, Hiwell Diatek, Wuxi, China). Furthermore, the 50% cytotoxicity concentration (CC_{50}), representing the drug concentration that reduced cell viability by 50%, was determined using GraphPad Prism 7.0 (GraphPad, San Diego, CA, USA).

Table 1. The Gradient elution procedure for HPLC.

Time (min)	Mobile phase A (methanol)	Mobile phase B (0.1% phosphoric acid)
0	3	97
5	3	97
35	33	67
40	37	63
45	46	54
65	90	10

As previously described (Liu et al. 2022), PIG1 cells were treated with α-MSH (100 nM; #CLP0120, Solarbio, Beijing, China) for 24 h to induce an *in vitro* model of hyperpigmentation. The model cells were then subjected to THSWD serum treatments at the selected appropriate concentrations for 48 h. The applied THSWD concentrations conformed to the previous study (Shi et al. 2023). Cells treated with the rat serum from the blank group served as control cells.

Melanin content assessment

The melanin content of PIG1 cells was assessed following the previously established protocol (Zhou and Sakamoto 2020). Briefly, PIG1 cells were seeded in a 6-well plate and harvested by trypsinization (trypsin, #T1300, Solarbio, Beijing, China). The supernatant was discarded after centrifugation at 1000 × g for 5 min. The cells were then lysed by adding 400 µL of NaOH solution (1 mol/L, #S5881, Sigma-Aldrich, MO, USA; containing 10% dimethyl sulfoxide) and heated in a metal bath at 70 °C for 1 h. Finally, the optical density (OD) was assessed at 490 nm on a microplate reader (DR-3518G, Hiwell Diatek, Wuxui, China).

Tyrosinase activity assessment

Tyrosinase activity was determined by assessing the levodopa (L-DOPA) oxidation rate. Briefly, PIG1 cells were seeded in a 6-well plate and collected by trypsinization. After centrifugation at 1000 × *g* for 5 min, the supernatant was removed for later use. Cells were lysed using 1% Triton X-100 solution (200 µL, #T8200, Solarbio) and stored at −80 °C for 30 min. The mixture was thawed at 37 °C and centrifuged at 3,000 × *g* for 30 min. Subsequently, 50 µL supernatant was seeded in a 96-well plate, and each well was added with 10 µL L-DOPA (#ID0360, Solarbio), followed by a 20 min incubation at 37 °C.

Western blotting

The total protein was separated from PIG1 cells using radioimmunoprecipitation assay (RIPA) lysis buffer (#P0013B, Beyotime, Shanghai, China) with phenylmethylsulfonyl fluoride (PMSF) protease inhibitor (#ST506, Beyotime), and the protein concentration was quantified using a bicinchoninic acid (BCA) kit (#P0010S, Beyotime). Proteins (25 µg/lane) were separated by 10% sodium dodecyl sulfate-polyacrylamide gel electrophoresis (SDS-PAGE; #P0015A, Beyotime) and transferred to polyvinylidene difluoride membranes (PVDF; #FFP24, Beyotime). The membranes were sealed with 5% nonfat milk (#P0216-300 g, Beyotime) for 1 h. The membranes were incubated overnight with primary antibodies at 4 °C and with goat anti-rabbit IgG H&L (HRP) secondary antibody (1: 2,000; #ab205718, Abcam, Cambridge, UK) for 1 h. Finally, an enhanced chemiluminescence (ECL) kit (#P1000, Pierce, Rockford, IL, USA) was used to visualize the membranes. Glyceraldehyde-3-phosphate dehydrogenase (GAPDH) served as a protein loading control. The primary and secondary antibodies used in Western blotting are presented in Table 2.

Statistical analysis

Statistical data analysis was conducted using GraphPad Prism version 7.0 (GraphPad Software). All data are presented as mean ± standard deviation. Tukey's *post hoc* test was used following a one-way analysis of variance (ANOVA) to determine the differences between the groups. $p < 0.05$ was considered statistically significant.

Results

Acquisition of THSWD-hyperpigmentation overlapping targets

After normalization using the PubChem database, 625 active ingredients of THSWD were identified in the HIT, TCMSP, and TCMID databases. Of these, 581 active ingredients met the screening criterion of having a QED score greater than 0.2 (Table S1). Subsequently, 733 targets associated with 153 active ingredients were collated, following the exclusion of ingredients lacking target information. Additionally, 3,111 hyperpigmentation-related targets were obtained from the GeneCards and DisGeNET databases. Ultimately, 323 overlap targets between THSWD and hyperpigmentation were identified using VennDiagram software, as illustrated in Figure 2(A). The network mapping THSWD-active ingredients to their corresponding targets is shown in Figure 2(B).

GO and KEGG pathway enrichment analyses

To elucidate the biological functions and pathways associated with the 323 potential targets, GO and KEGG pathway enrichment analyses were performed. GO analysis revealed that these targets were involved in 2,522 BP terms, 156 CC terms, and 52 MF terms ($p < 0.01$, Table S2). Subsequently, the top five enriched GO terms were selected from each of the BP, CC, and MF categories. These targets were predominantly associated with biological processes such as 'response to peptide' (GO: 1901652; count = 73) and 'response to lipopolysaccharide' (GO: 0032496; count = 61), cellular components such as 'vesicle lumen' (GO: 0031983; count = 36) and 'cytoplasmic vesicle lumen' (GO: 0060205; count = 35), and molecular functions including 'receptor ligand activity' (GO: 0048018; count = 57) and 'signalling receptor activator activity' (GO: 0030546; count = 57), among others. These findings are presented in Figure 3 and Table 3.

The KEGG pathway analysis identified 167 enriched pathways, which were categorized into various groups: 25 pathways

Table 2. Primary and secondary antibodies used in Western blotting.

Name	Species	UniProt ID	Dilution	RRID number	Catalogue number	Supplier
ALB Antibody	Rabbit	P02768	1:1000	AB_2838359	DF6396	Affinity
IL6 Antibody	Rabbit	P05231	1:1000	AB_2838055	DF6087	Affinity
MAPK3 Antibody	Rabbit	P27361/P28482	1:1000	AB_2833336	AF0155	Affinity
p-MAPK3 Antibody	Rabbit	P27361/P28482	1:1000	AB_2834432	AF1015	Affinity
MITF Antibody	Rabbit	O75030	1:1000	AB_2834960	AF6027	Affinity
MC1R Antibody	Rabbit	Q01726	1:1000	AB_2837351	DF4992	Affinity
GAPDH Antibody	Rabbit	P04406	1:1000	AB_561053	2118	CST
Goat Anti-Rabbit IgG H&L (HRP)	Goat	N/A	1:2000	AB_2819160	ab205718	Abcam

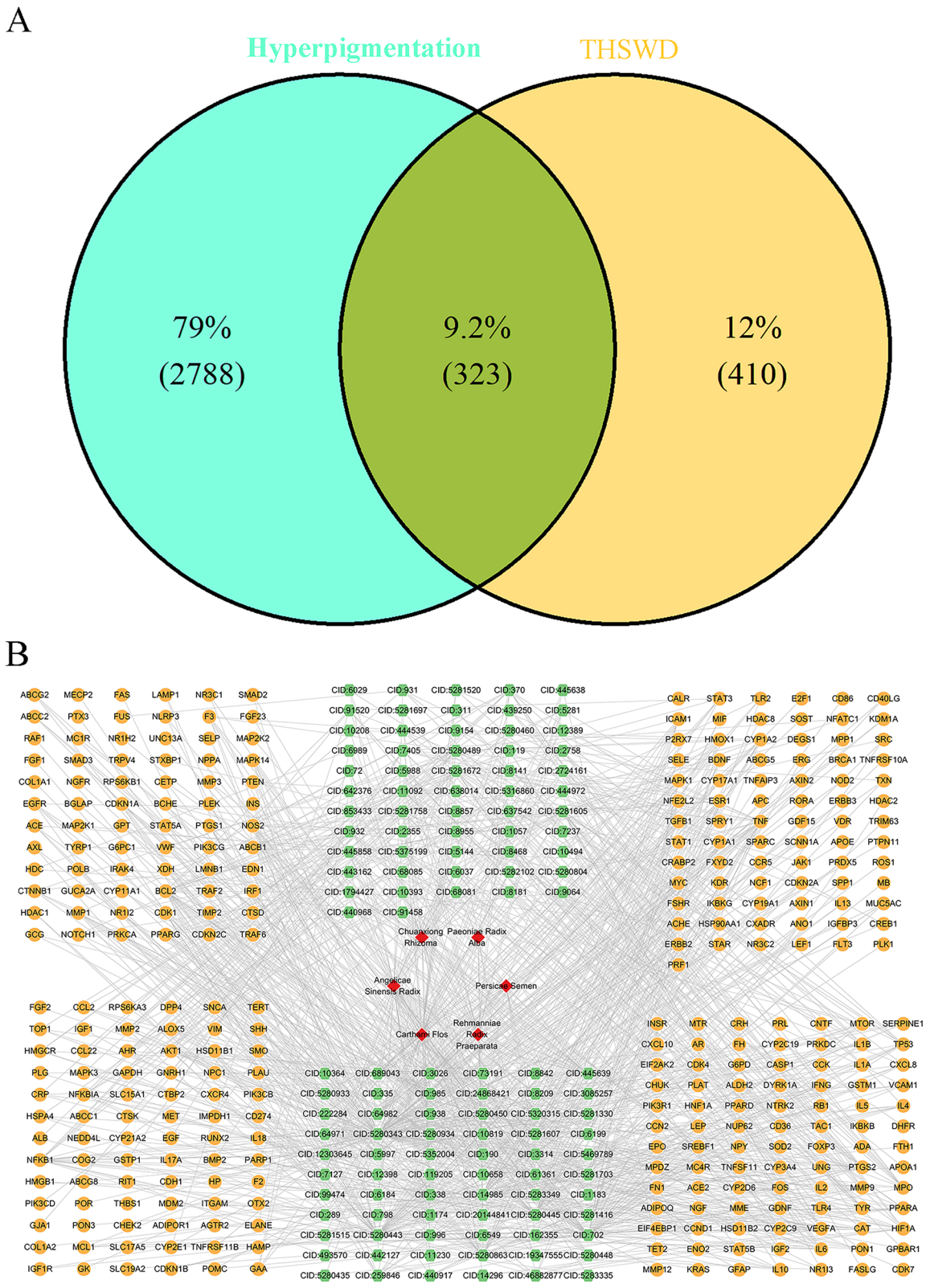

Figure 2. Venn diagram of the THSWD-hyperpigmentation overlapping targets (A) and the THSWD-active ingredient-target network, constructed by cytoscape (B). THSWD, Tao-Hong-Si-Wu decoction.

were related to environmental information processing (Figure 4(A)), 65 pathways to human diseases (Figure 4(B)), 49 pathways to organismal systems (Figure 4(C)), 12 pathways to cellular processes (Figure 5(A)), four pathways to metabolism (Figure 5(B)), and 12 pathways to other categories (Figure 5(C)), all with a p-value < 0.01. The analysis highlighted that the potential targets were predominantly involved in key pathways, particularly the PI3K-Akt signaling pathway (hsa04151; count = 68) and the MAPK signalling pathway (hsa04010; count = 47). Details of all enriched pathways are presented in Table S3.

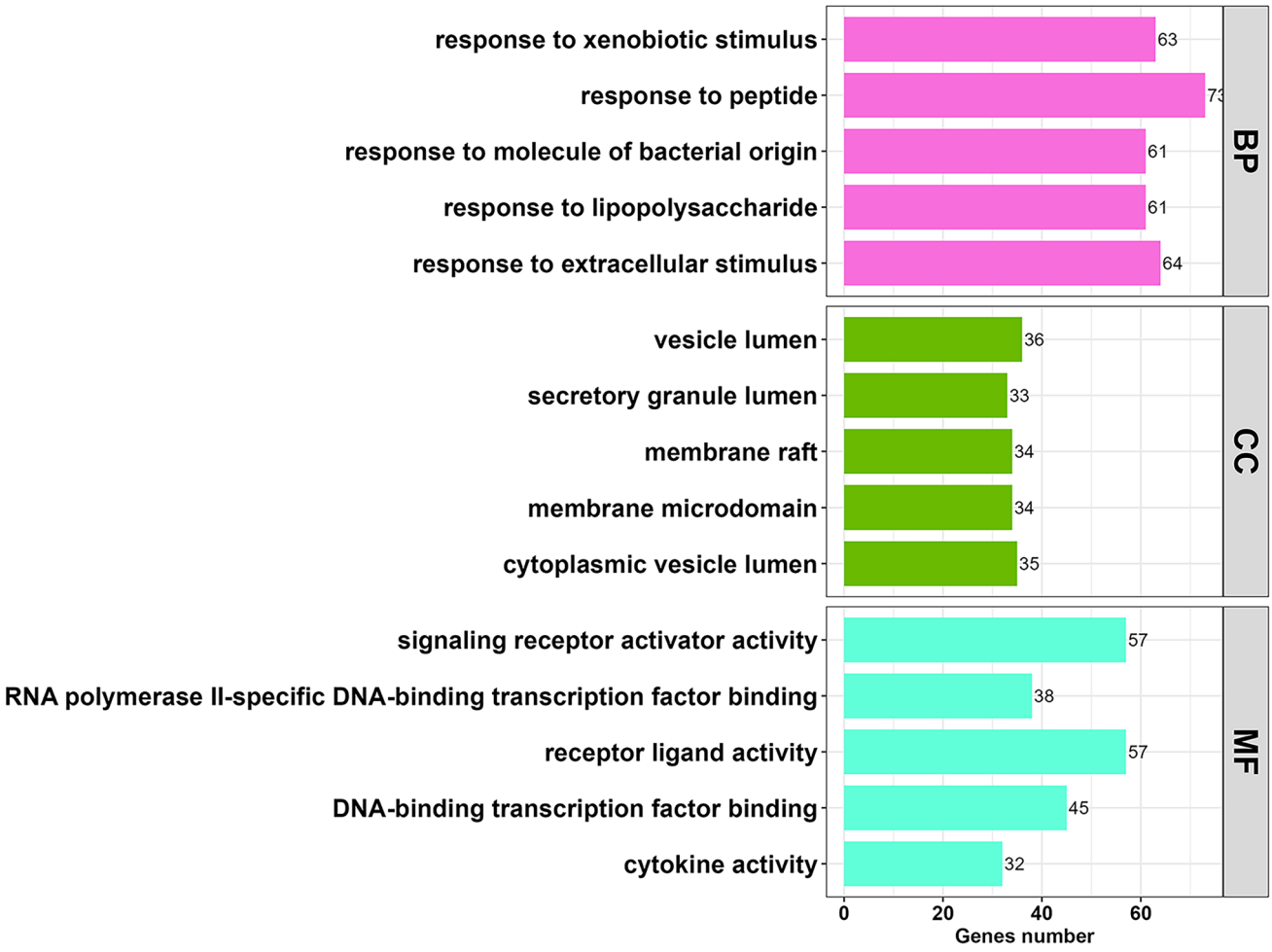

Figure 3. Histogram of 15 vitally enriched GO terms, including the top 5 BPs, CCs, and MFs. GO analysis was conducted using clusterProfifiler. *P* value < 0.01. GO: gene ontology; BP: biological process; CC: cellular component; MF: molecular function.

Table 3. Top 5 enriched BP, CC, and MF terms in GO enrichment analysis.

ONTOLOGY	ID	Description	*p* value	Count
BP	GO:1901652	response to peptide	2.02E-47	73
BP	GO:0032496	response to lipopolysaccharide	5.25E-45	61
BP	GO:0002237	response to molecule of bacterial origin	2.36E-43	61
BP	GO:0009410	response to xenobiotic stimulus	1.38E-41	63
BP	GO:0009991	response to extracellular stimulus	1.62E-38	64
CC	GO:0031983	vesicle lumen	1.61E-19	36
CC	GO:0060205	cytoplasmic vesicle lumen	1.08E-18	35
CC	GO:0045121	membrane raft	9.40E-18	34
CC	GO:0098857	membrane microdomain	1.03E-17	34
CC	GO:0034774	secretory granule lumen	4.95E-17	33
MF	GO:0048018	receptor ligand activity	1.44E-30	57
MF	GO:0030546	signaling receptor activator activity	3.07E-30	57
MF	GO:0140297	DNA-binding transcription factor binding	1.13E-20	45
MF	GO:0061629	RNA polymerase II-specific DNA-binding transcription factor binding	1.57E-19	38
MF	GO:0005125	cytokine activity	1.81E-19	32

PPI network analysis of overlapping targets and THSWD-active ingredient-hub target-pathway network construction

To establish a PPI network, the 323 overlapping targets were placed into the STRING database. The resulting PPI network consisted of 330 nodes, representing proteins with a degree of one or higher, and 10,371 edges, signifying interactions with a score greater than 0.4 (Figure 6(A)). Subsequently, the MNC (Figure 6(B)), MCC (Figure 6(C)), and EPC (Figure 6(D)) methods of cytoHubba were used to identify the top 20 targets within the PPI network. This analysis led to the identification of 11 overlapping targets, which were considered as the hub targets (Figure 7(A)). The key targets included albumin (ALB), interleukin 6 (IL6), vascular endothelial growth factor A (VEGF-A), glyceraldehyde-3-phosphate dehydrogenase (GAPDH), signal transducer and activator of transcription 3 (STAT3), AKT serine/threonine kinase 1 (AKT1), insulin (INS), tumour necrosis factor (TNF), interleukin 1 beta (IL1B), epidermal growth factor (EGF), and mitogen-activated protein kinase 3 (MAPK3), as detailed in Table 4.

The THSWD-active ingredient-hub target-pathway network analysis revealed that THSWD primarily influences these hub targets through pathways such as the Ras and Rap1 signalling pathways (Figure 7(B)). Additionally, the top five active ingredients within this network were identified using the radiality, degree, closeness centrality, and betweenness centrality methods in Cytoscape. This process resulted in the identification of three overlapping active ingredients: quercetin, apigenin, and luteolin (Figure 7(C)). Consequently, quercetin, apigenin, and luteolin were recognized as key active ingredients in THSWD to combat hyperpigmentation and selected for further analysis.

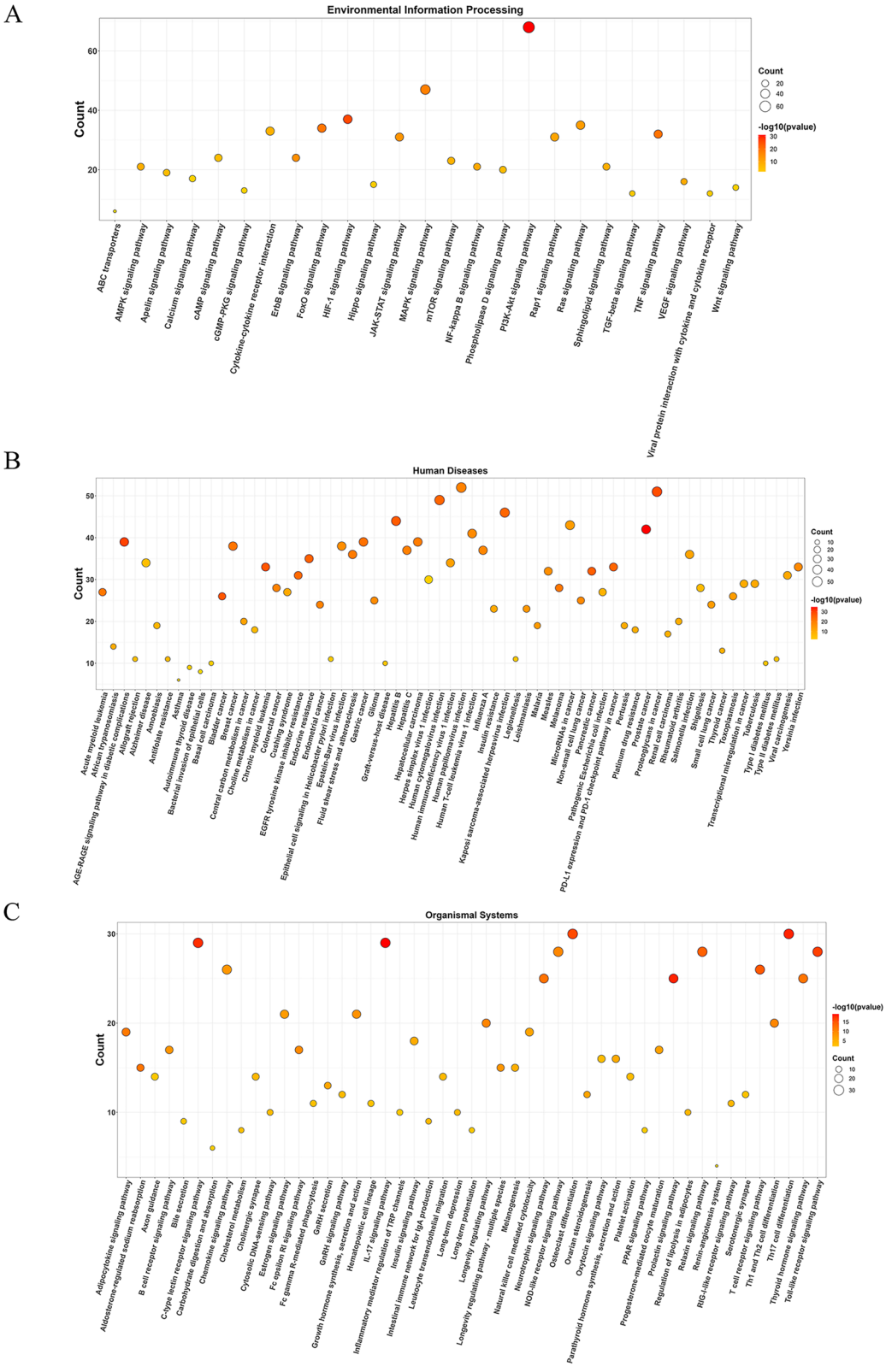

Figure 4. Bubble diagrams of the enriched KEGG pathways, including 25 terms belonging to environmental information processing (a), 65 to human diseases (B), and 49 to organismal systems (C). KEGG analysis was conducted using clusterProfifiler. *P* value < 0.01. KEGG: Kyoto encyclopedia of genes and genomes.

MR analysis

Through Mendelian randomization analysis, we identified three targets, ALB, IL6, and MAPK3, that showed a significant association with the risk of hyperpigmentation (Figure 8(A,B)). Applying the IVW method, ALB (95% confidence interval [CI]: 0.573–1.047) with an odds ratio (OR) of 0.774, IL6 (95% CI: 0.507–0.907) with an OR of 0.678, and MAPK3 (95% CI: 1.041–1.269) with an OR of 1.149 were all significantly associated with hyperpigmentation risk (Figure 8(C)). The funnel plots demonstrated a

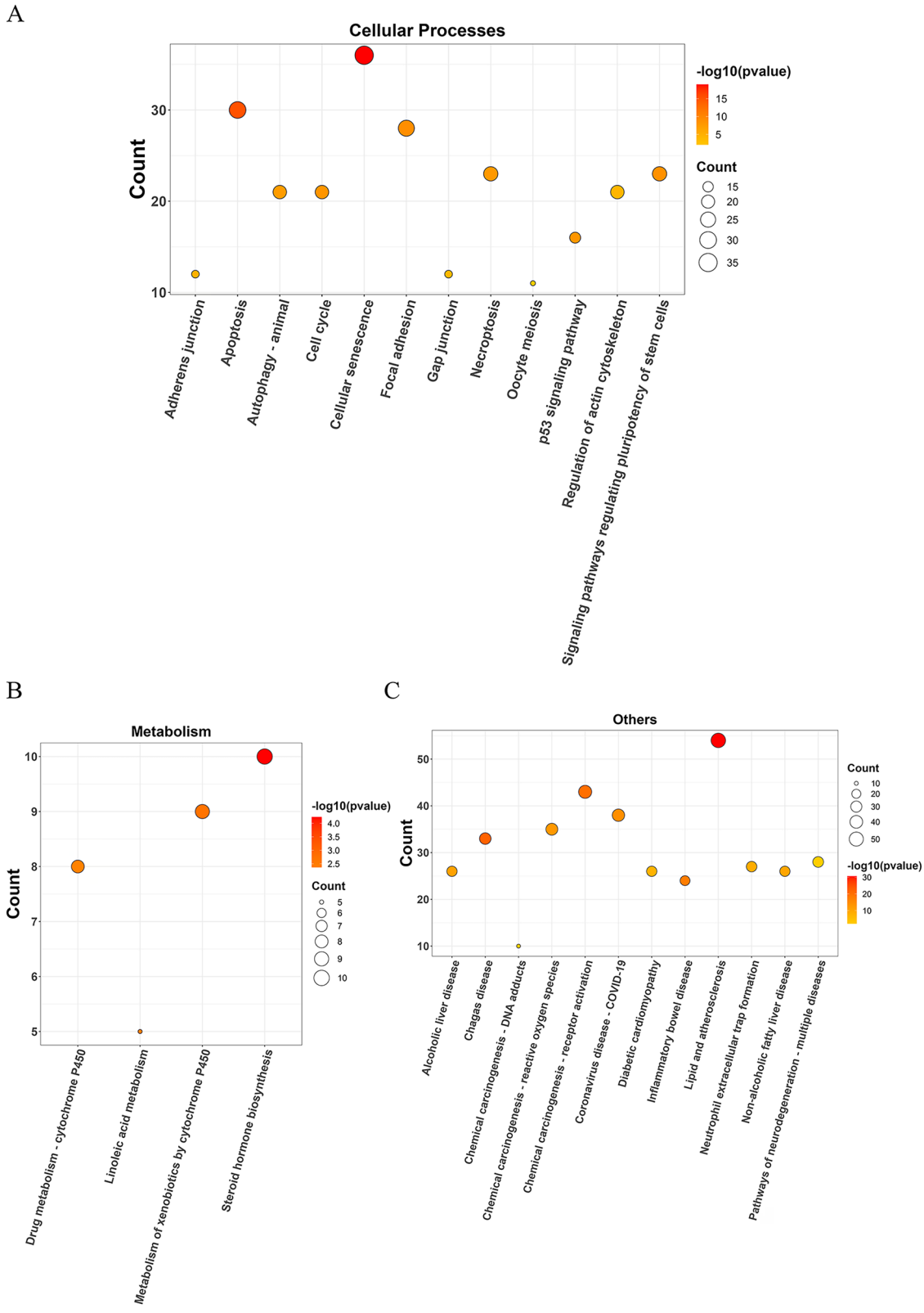

Figure 5. Bubble diagrams of the enriched KEGG pathways, including 12 terms belonging to cellular processes (a), 4 to metabolism (B), and 12 to others (C). KEGG analysis was conducted using clusterProfifiler. *P* value < 0.01. KEGG: Kyoto encyclopedia of genes and genomes.

roughly symmetrical distribution, indicating consistency in the causal effects (Figure 8(C)). Consequently, ALB, IL6, and MAPK3 were established as the primary anti-hyperpigmentation targets of THSWD for subsequent analyses.

Molecular docking verification

To verify the reliability of the identified potential targets for THSWD in treating hyperpigmentation, molecular docking was performed between the core active ingredients and the hub targets. The three

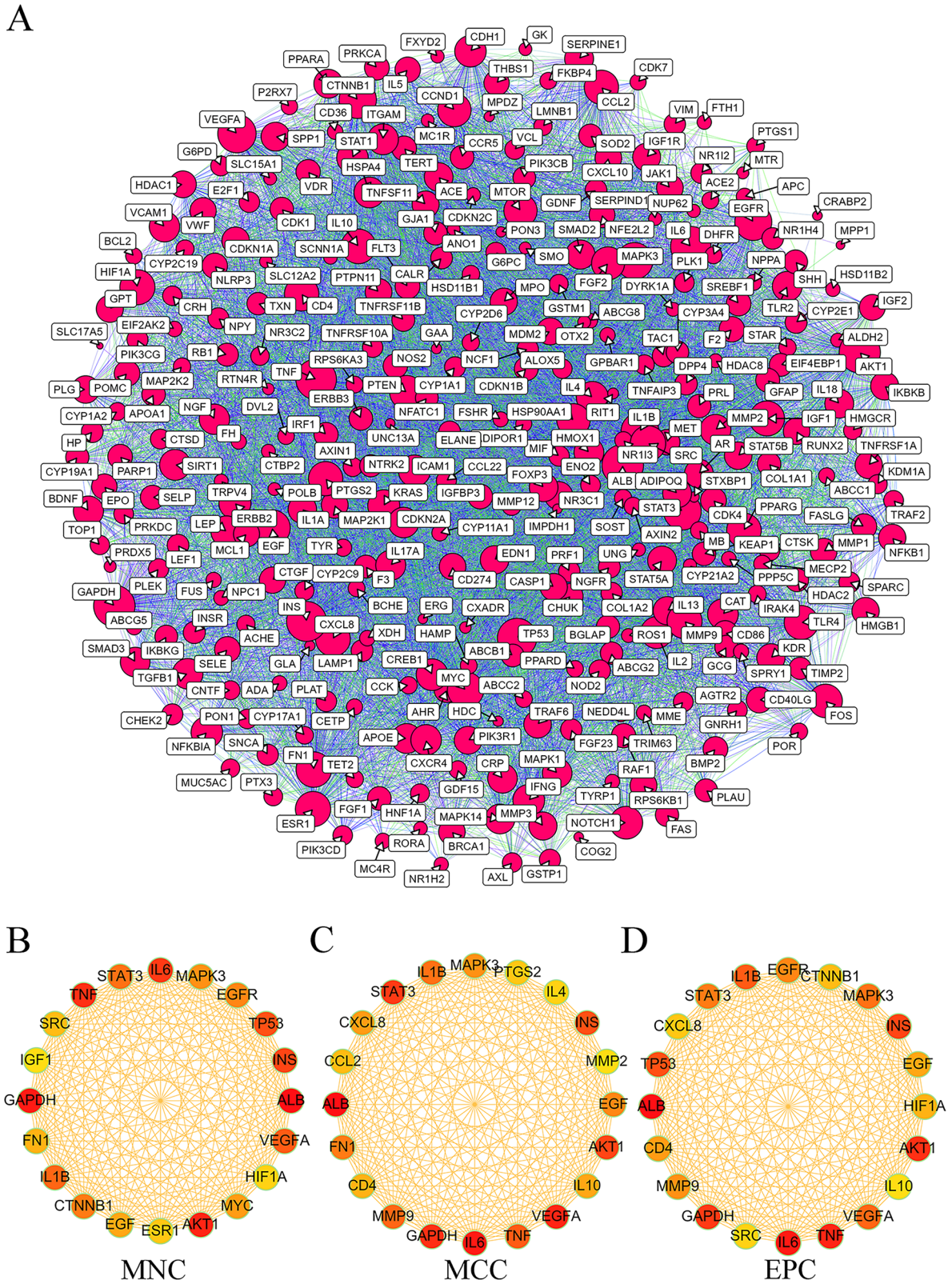

Figure 6. PPI network analysis of THSWD-hyperpigmentation overlapping targets. (A) PPI network, built by STRING database and visualized by cytoscape. (B-D) Selection of the top 20 hub targets from the PPI network using MNC, MCC, and EPC methods of cytoHubba. PPI: protein-protein interaction; THSWD: Tao-Hong-Si-Wu decoction; STRING: Search Tool for the Retrieval of Interacting genes/proteins; MNC: maximum neighborhood component; MCC: maximal clique centrality; EPC: edge percolated component.

primary active ingredients, quercetin, apigenin, and luteolin, were docked with the three key targets: ALB, IL6, and MAPK3. The results showed that quercetin exhibited a strong binding affinity with ALB (binding energy = −7.8 kcal/mol), IL6 (binding energy = −7.1 kcal/mol), and MAPK3 (binding energy = −9.2 kcal/mol) (Figure 9(A–C) and Table 5). Apigenin showed favourable binding interactions with IL6 (binding energy = −6.8 kcal/mol) and MAPK3 (binding energy = −9.2 kcal/mol) (Figure 9(D–E) and Table 5). Luteolin showed a

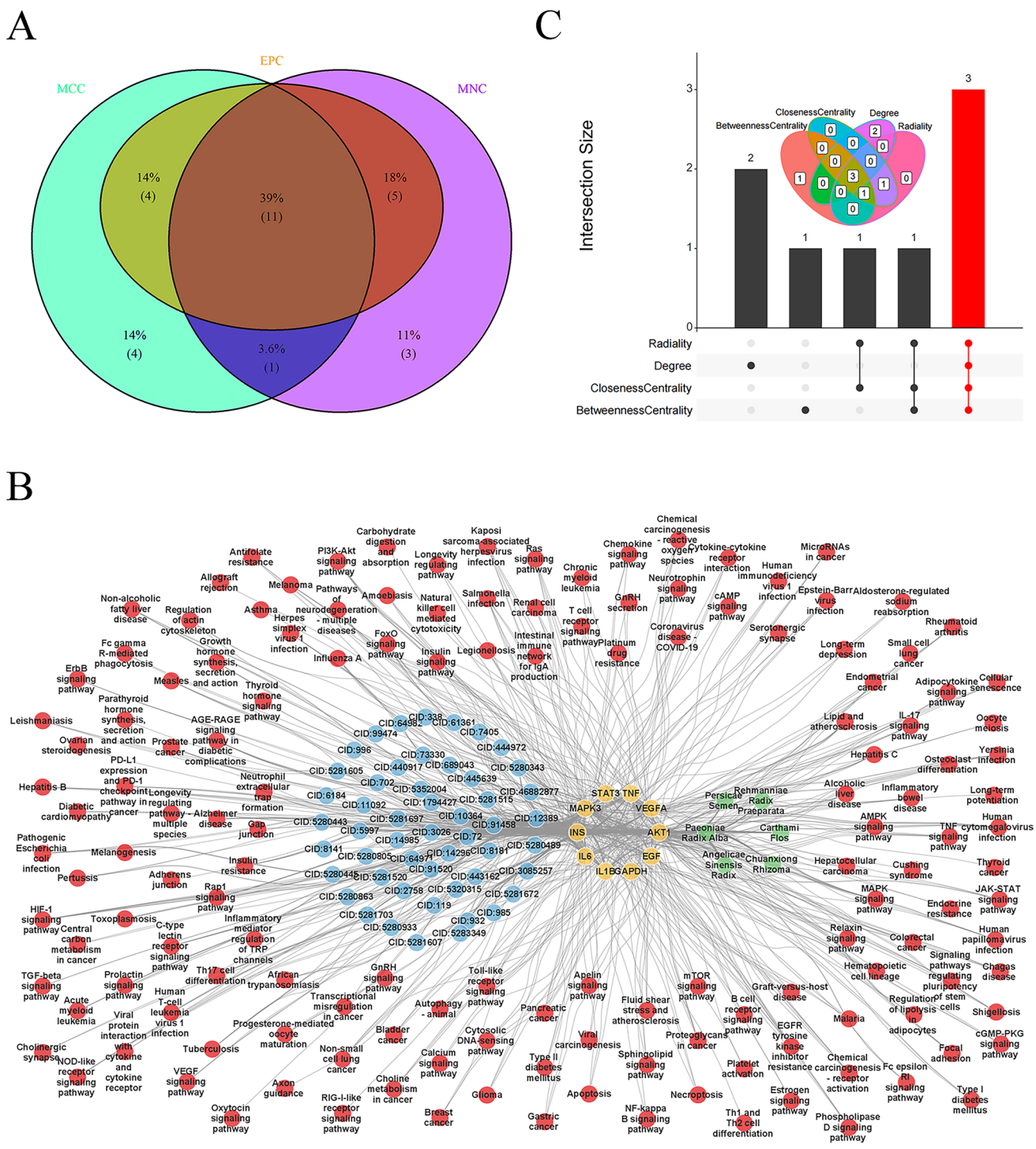

Figure 7. Screening the core targets and active ingredients. Venn diagram of overlapping hub targets based on MNC, MCC, and EPC methods (A), THSWD-active ingredient-hub target-pathway network, constructed by cytoscape (B), and overlapping core active ingredients screened by radiality, degree, closeness centrality, and betweenness centrality methods using UpSetR package (C). MNC: maximum neighborhood component; MCC: maximal clique centrality; EPC: edge percolated component; THSWD: Tao-Hong-Si-Wu decoction.

significant binding affinity with ALB (binding energy = −9.5 kcal/mol), IL6 (binding energy = −7.2 kcal/mol), and MAPK3 (binding energy = −9.3 kcal/mol) (Figure 9(F–H) and Table 5).

HPLC analysis and in vitro verification

HPLC analysis identified three active ingredients in THSWD: quercetin, apigenin, and luteolin (Figure 10(A)). Chromatographic peaks corresponding to these ingredients were observed at different retention times. Specifically, quercetin was detected at 53.379 min, luteolin at 54.570 min, and apigenin at 56.893 min (Figure 10(A)).

A CCK-8 assay was performed to establish the appropriate THSWD treatment concentrations for PIG1 cells. The results indicated that concentrations of 2.5%, 5%, 10%, 15%, and 20% were suitable, with a half-maximal cytotoxic concentration (CC_{50}) of 32.14% (Figure 10(B,C)). Consequently, these five concentrations of THSWD were selected for use in subsequent assays.

Table 4. The top 11 hub targets from the PPI network.

Target	MNC score	MCC score	EPC score
ALB	235	1.03E+46	16.105
IL6	220	1.03E+46	15.679
VEGFA	194	1.03E+46	14.121
GAPDH	233	1.03E+46	15.081
STAT3	186	1.03E+46	13.346
AKT1	231	1.03E+46	15.172
INS	215	1.03E+46	14.554
TNF	222	1.03E+46	15.361
IL1B	187	1.03E+46	14.226
EGF	166	1.03E+46	13.033
MAPK3	176	1.03E+46	13.528

To further investigate the anti-hyperpigmentation effect of THSWD, an *in vitro* model was established by treating PIG1 cells with α-MSH, as per the methodology outlined in a previous study (Liu et al. 2022). Tyrosinase, a key enzyme in melanin synthesis, serves as a direct indicator of melanin production efficacy (Zhou and Sakamoto 2020). Our data revealed that both the melanin content and the tyrosinase activity increased significantly in α-MSH-induced PIG1 cells compared to control cells ($p < 0.01$). This upregulation was markedly reversed after THSWD treatment ($p < 0.05$; Figure 10(D,E)).

Additionally, we examined the expression of two hyperpigmentation-related proteins, MC1R and MITF, in PIG1 cells. MC1R, located on the surface of melanocytes, activates a signalling cascade involving MITF, leading to the transcription of melanin synthesis genes (Li et al. 2022). In our study, the protein expression levels of MC1R and MITF were significantly elevated in α-MSH-induced PIG1 cells compared to control cells ($p < 0.01$), but these increases were mitigated by THSWD treatment ($p < 0.05$; Figure 10(F)).

Furthermore, we assessed the expression levels of three key targets, ALB, IL6, and MAPK3, in PIG1 cells to understand the specific regulatory effects of THSWD on hyperpigmentation. We observed that protein expression levels of ALB and *p*-MAPK3/MAPK3 were significantly reduced, while IL6 levels were markedly increased in α-MSH-induced PIG1 cells compared to control cells ($p < 0.01$; Figure 10(G)). However, THSWD treatment reversed the α-MSH-induced changes in protein expression levels of ALB, IL6, and the p-MAPK3/MAPK3 ratio in PIG1 cells ($p < 0.05$; Figure 10(G)).

Discussion

Hyperpigmentation is a common disorder and a source of cosmetic concern, potentially causing psychological distress, reduced productivity, and decreased quality of life (Boo 2019; Wenner and Ramberg 2022). The pathological mechanisms underlying hyperpigmentation are complex, with inflammation (Fu et al. 2020) and oxidative stress (Xing et al. 2022) identified as key factors influencing melanogenesis and contributing to its pathogenesis. THSWD is a classic TCM formula renowned for promoting blood circulation and nourishing blood. It exhibits various pharmacological activities, notably anti-inflammatory and antioxidant properties (Shao et al. 2022). Recently, *Paeoniae Radix Alba*, a component of THSWD, has been recognized as a significant TCM agent against pigmentation (Guo et al. 2021). However, the specific effects of THSWD on hyperpigmentation and its underlying mechanisms remain largely unexplored. This study aims to elucidate the anti-hyperpigmentation mechanisms of THSWD through network pharmacology analysis.

In this study, we identified 581 active ingredients of THSWD following ADME screening. Subsequently, 733 targets related to THSWD and 3,111 targets associated with hyperpigmentation were obtained. From these, 323 overlapping targets between THSWD and hyperpigmentation were selected for further analysis.

The pathophysiology of hyperpigmentation is primarily characterized by abnormal melanin overproduction (Kumari et al. 2018). The process of melanin production begins when keratinocytes release α-MSH, which binds to the MC1R receptor, leading to activation of adenylate cyclase and subsequent cAMP synthesis (Yun et al. 2015). This cascade triggers CREB phosphorylation and activates the MITF promoter (Yun et al. 2015). Increased MITF expression enhances the expression of tyrosinase, the key rate-limiting enzyme in melanin synthesis, thus facilitating melanin production in melanocytes (Sun et al. 2017; Zhou and Sakamoto 2020). Given this mechanism, targeting tyrosinase activity to reduce melanogenesis is considered a safe and effective strategy to treat hyperpigmentation (Mann et al. 2018).

GO analysis of the 323 candidate targets revealed a significant concentration in BPs such as the response to peptide and the response to lipopolysaccharide. Peptides are known to play a crucial role in melanogenesis (Honisch et al. 2022). For example, glutathione, a notable antioxidant, can inhibit melanin synthesis by directly reducing tyrosinase activity, thus offering potential in hyperpigmentation treatment (Lu and Tonissen et al. 2021). Furthermore, lipopolysaccharide has been shown to stimulate melanin and inflammatory factor production in cells (Ding et al. 2020). THSWD has been reported to effectively mitigate inflammation, helping restore damaged skin tissues (Zhou et al. 2018; Zhang et al. 2023). Additionally, the candidate targets were enriched in CCs, such as the vesicle lumen, and MFs, such as receptor ligand activity. In the endomembrane system, over 30% of protein location in eukaryotic cells occurs within membrane-enclosed organelles, and vesicles play a crucial role in the trafficking of membrane proteins (Menasche et al. 2019). In melanogenesis, Rab32 and Rab38, key modulators of vesicular trafficking, are involved in melanin production (Ambrosio and Di Pietro 2017). Furthermore, receptor-ligand interactions are significantly involved in melanogenesis. For example, the upregulation of LXR-α of beauvericin, a nuclear receptor, suggests its potential as a hyperpigmentation inhibitor (Lee et al. 2018). These findings suggest that THSWD may exert its therapeutic effects on hyperpigmentation primarily by regulating various biological activities, including response to peptides and lipopolysaccharides, vesicle trafficking, and receptor-ligand interactions.

The KEGG pathway analysis revealed that candidate targets are significantly associated with pathways such as PI3K-Akt and MAPK signalling. Growing evidence suggests that these pathways play a critical role in the onset and progression of hyperpigmentation disorders (Nishina et al. 2018; Chaiprasongsuk and Panich 2022). For example, it has been shown that the PI3K-Akt axis influences GSK3β phosphorylation at Ser9, which in turn inhibits the activity of MITF, a key regulator of tyrosinase gene expression, ultimately resulting in reduced melanogenesis in melanoma cells (Zhou and Sakamoto 2019). MAPKs, including JNK, ERK, and p38 MAPK, are essential signaling molecules in melanogenesis regulation (Sun et al. 2020). A recent study showed that activation of the p38 MAPK signalling pathway could stimulate melanin production in human epidermal melanocytes (Xu et al. 2018). NED-180, a synthetic *Piper* amide derivative, was found to suppress MITF phosphorylation by activating the PI3K/Akt and ERK pathways, thus reducing hyperpigmentation in guinea pigs (Hwang et al. 2016). These insights

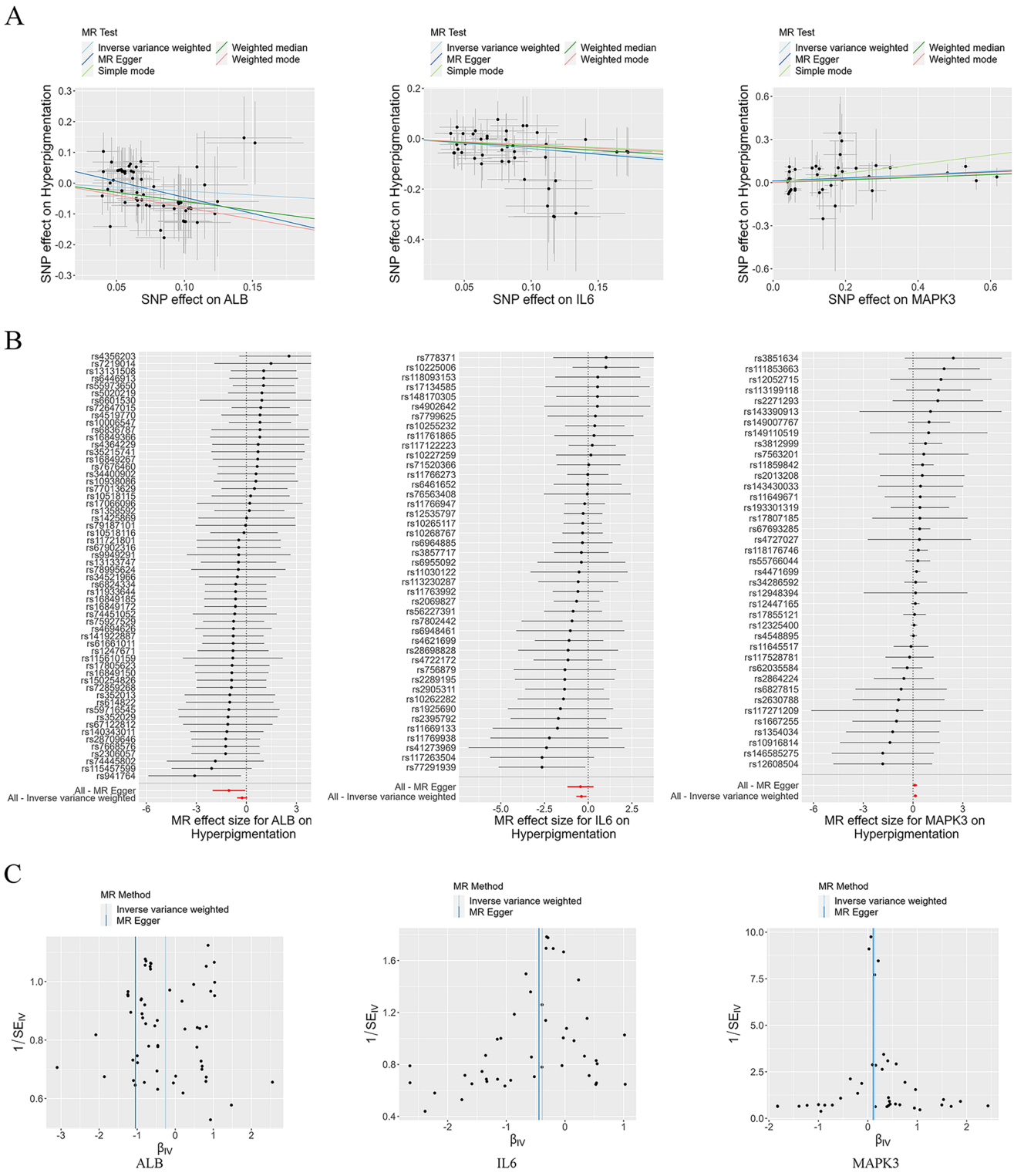

Figure 8. Mendelian Randomization analysis. Scatter plots demonstrating the causal effects of ALB, IL6, and MAPK3 on the risk of hyperpigmentation (a), Forest plots demonstrating the causal effects of ALB, IL6, and MAPK3 each SNP on the risk of hyperpigmentation (B), and funnel plots demonstrating the overall heterogeneity of MR estimates for the effects of ALB, IL6, and MAPK3 on hyperpigmentation (C). ALB: albumin; MAPK3: mitogen-activated protein kinase 3; SNP: single nucleotide polymorphism; MR: Mendelian randomization.

suggest that THSWD may effectively counteract hyperpigmentation primarily by modulating the PI3K-Akt and MAPK signalling pathways, which are crucial in melanogenesis. This hypothesis underscores the need for more research to elucidate the specific roles of these pathways in the anti-hyperpigmentation mechanisms of THSWD.

PPI network analysis identified ALB, IL6, VEGFA, GAPDH, STAT3, AKT1, INS, TNF, IL1B, EGF, and MAPK3 as the core targets of THSWD in counteracting hyperpigmentation. Subsequently, we constructed a THSWD-active ingredient-hub target-pathway network, through which quercetin, apigenin, and luteolin were determined as the primary active ingredients. This

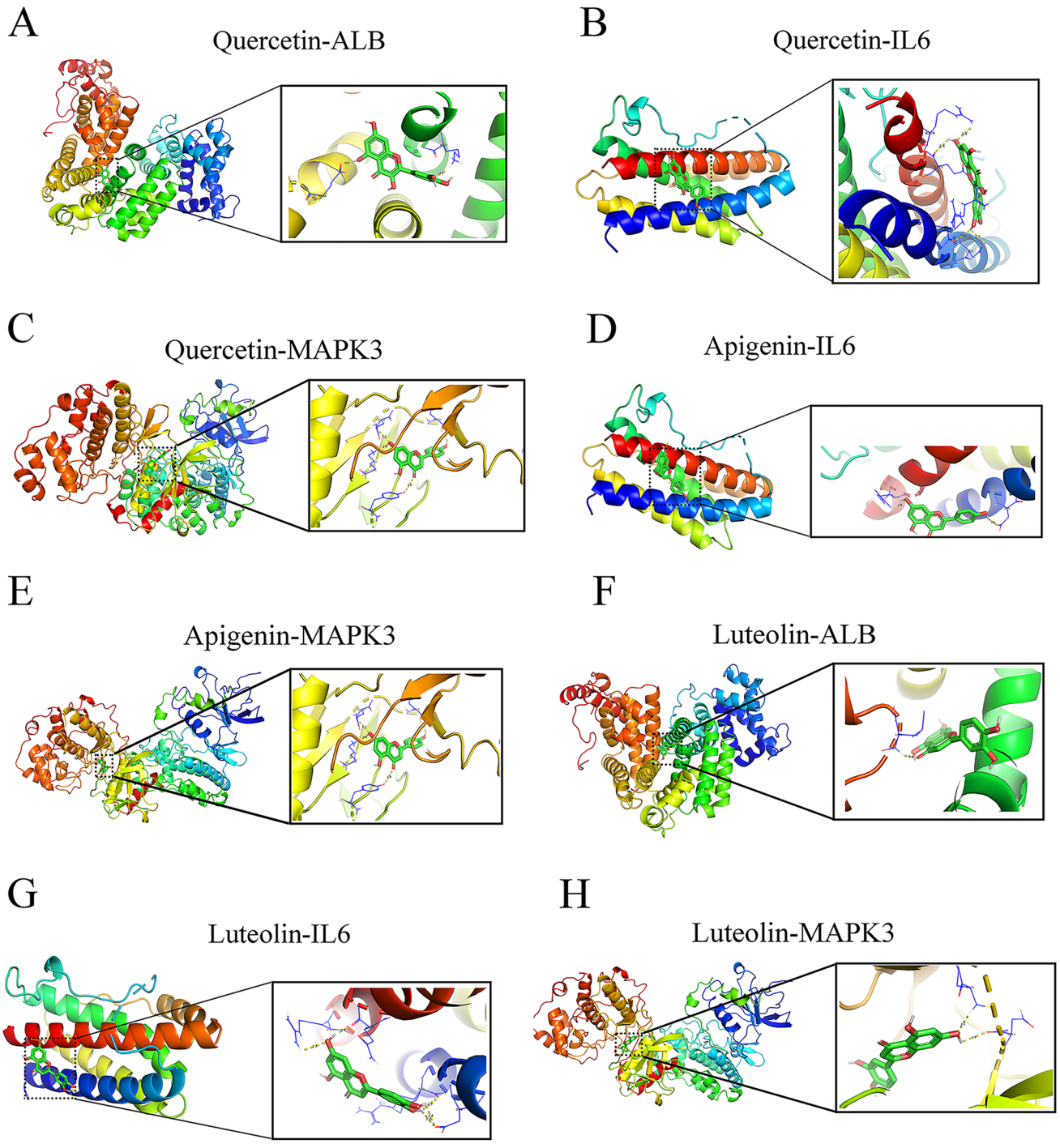

Figure 9. Molecular docking modes. Quercetin-ALB (a), quercetin-IL6 (B), quercetin- MAPK3 (C), apigenin-IL6 (D), apigenin-MAPK3 (E), luteolin-ALB (F), luteolin -IL6 (G), and luteolin-MAPK3 (H). Binding energy < -5 kcal/mol. ALB: albumin; MAPK3: mitogen-activated protein kinase 3.

Table 5. Results of molecular docking.

Target	Pubchem_ID	Compound	Binding energy (kcal/mol)
ALB	CID:5280343	Quercetin	−7.8
ALB	CID:5280445	Luteolin	−9.5
IL6	CID:5280343	Quercetin	−7.1
IL6	CID:5280443	Apigenin	−6.8
IL6	CID:5280445	Luteolin	−7.2
MAPK3	CID:5280343	Quercetin	−9.2
MAPK3	CID:5280443	Apigenin	−9.2
MAPK3	CID:5280445	Luteolin	−9.3

identification was achieved by integrating methods such as radiality, degree, closeness centrality, and betweenness centrality. Furthermore, HPLC analysis confirmed quercetin, apigenin, and luteolin as active ingredients. In particular, the Mendelian randomization analysis revealed a significant association between the three hub targets, ALB, IL6, and MAPK3, and the risk of hyperpigmentation. Consequently, these primary active ingredients, quercetin, apigenin, and luteolin, together with the key targets, ALB, IL6, and MAPK3, were selected for further investigation and validation.

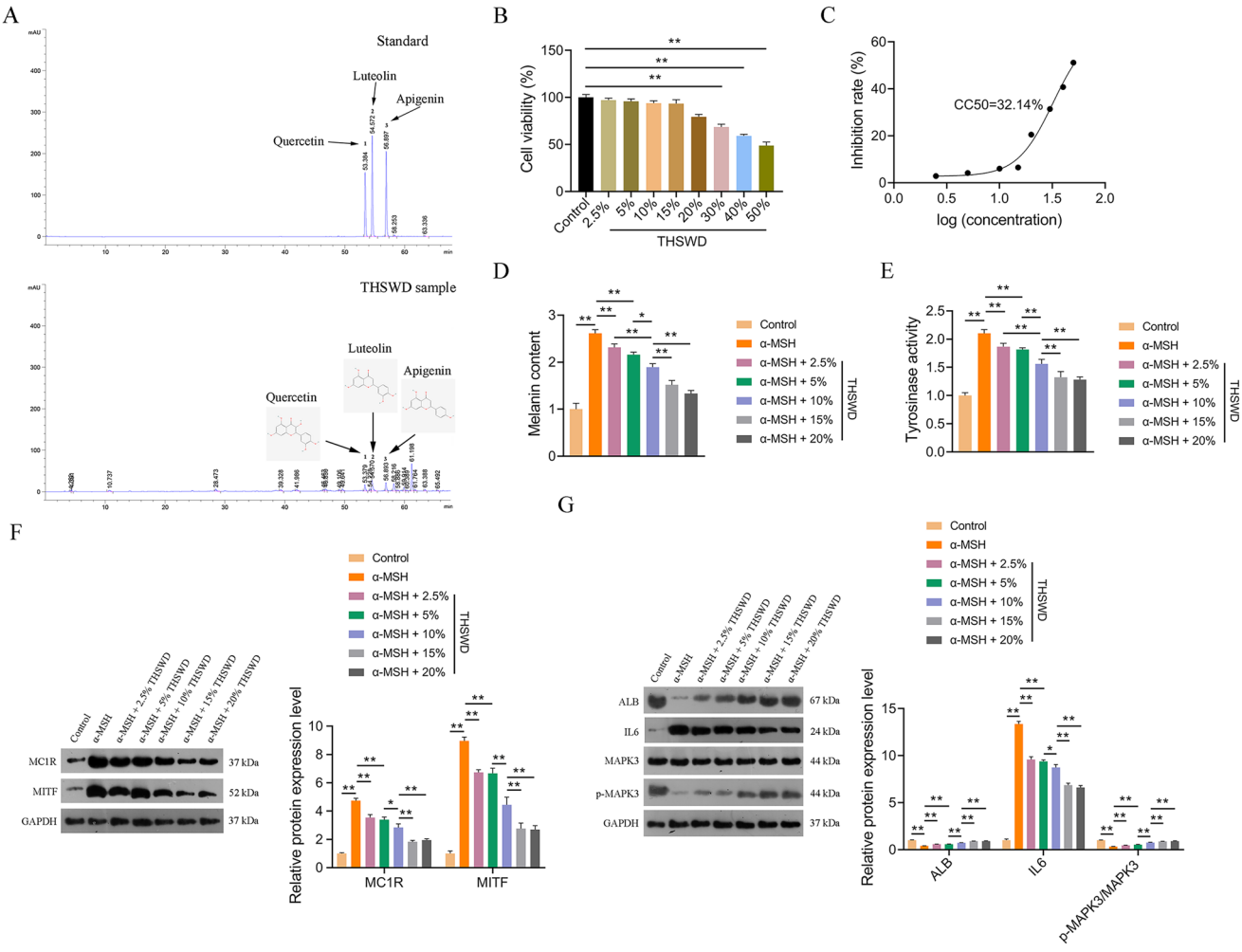

Figure 10. HPLC analysis and *in vitro* verification. Quality control and identification of key active ingredients of THSWD through HPLC analysis (a), determination of suitable treatment concentrations of THSWD (B), quantification of the CC_{50} of THSWD for PIG1 cells (C), assessment of melanin contents (D), assessment of tyrosinase activity (E), assessment of the expression of hyperpigmentation-related proteins, MC1R and MITF (F), and assessment of the expression of key targets, ALB, IL6, and MAPK3 (G). F-G: Protein expression levels were detected by Western blotting. Initially, the CCK-8 assay was used to investigate and determine the appropriate concentrations of THSWD treatment for subsequent assays. PIG1 cells were exposed to prepared serum THSWD (from SD rats) at gradient concentrations (2.5%, 5%, 10%, 15%, 20%, 30%, 40%, and 50%) for 24 h. PIG1 cells were treated with 100 nM α-MSH for 24 h to induce an *in vitro* model of hyperpigmentation. The model cells were treated with the appropriate concentrations of serum THSWD (2.5%, 5%, 10%, 15%, and 20%) determined for 48 h. All data are shown as mean ± standard deviation. $^{*}p < 0.05$ and $^{**}p < 0.01$. HPLC: high performance liquid chromatograph; CCK-8: cell counting kit-8; THSWD: Tao-Hong-Si-Wu decoction; CC50: 50% cytotoxicity concentration; ALB: albumin; MAPK3: mitogen-activated protein kinase 3.

Molecular docking studies revealed that quercetin, apigenin, and luteolin possess favorable binding affinities with ALB, IL6, and/or MAPK3. As the most abundant plasma protein, ALB plays a vital role in regulating blood plasma colloid osmotic pressure and functions as a carrier for various substances, including fatty acids, hormones, and drugs (Shi et al. 2022). IL6, a well-known pro-inflammatory cytokine, has been observed to upregulate in keratinocytes during ultraviolet radiation-induced hyperpigmentation. The involvement of MAPK3 in melanin regulation in hyperpigmentation is plausible, especially considering that targeting the MAPK signaling pathway can inhibit melanogenesis (Chae et al. 2017)

Quercetin, luteolin, and apigenin are members of the flavonoid family, commonly found in plants, and are known for their antioxidant and anti-inflammatory properties (Imran et al. 2019; Wu et al. 2021; Di Petrillo et al. 2022). Luteolin has been shown to inhibit pro-inflammatory factors such as IL-6, TNF-α, and IL1B, thereby reducing skin inflammation (Gendrisch et al. 2021). ALB has been identified as a core target of luteolin in combating inflammation, and the PI3K-Akt and Ras signaling pathways are critical in this context (Huang et al. 2020). Previous research has demonstrated that quercetin and luteolin can downregulate IL-6 and other pro-inflammatory mediators in macrophages and inhibit melanogenesis in melanocytes (Ma et al. 2021). Moreover, these flavonoids are known to influence tyrosinase activity, impacting auto-oxidation, enzymatic oxidation, and melanogenesis (Lu et al. 2021). Recent research has shown that quercetin 3-*O*-galactoside, a derivative of quercetin, can suppress melanogenesis by modulating PKA/MITF signaling and ERK activation, indicating its potential as a cosmetic ingredient against hyperpigmentation (Karadeniz et al. 2023).

Intriguingly, *in vitro* experiments demonstrated the anti-hyperpigmentation effects of THSWD. Following THSWD treatment, both melanin content and tyrosinase activity showed a marked reduction in the hyperpigmentation cell model. Additionally, the expression levels of MC1R and MITF, key regulators of melanin synthesis (Li et al. 2022), were significantly downregulated after THSWD treatment. Regarding the impact on primary targets, THSWD treatment led to increased protein

expression levels of ALB and p-MAPK3/MAPK3, while decreasing protein expression levels of IL6. Previous research has indicated that ALB can protect tissues from inflammatory damage (Duran-Güell et al. 2021), and MAPK3 has been implicated in melanin synthesis (Yan et al. 2023). Moreover, IL6 overexpression has been associated with skin hyperpigmentation after intravenous polymyxin B treatment (Mattos et al. 2017). Collectively, these results suggest that the therapeutic efficacy of THSWD against hyperpigmentation may be attributed to its regulatory effects on ALB, IL6, and MAPK3.

This study has several limitations. First, our findings are highly dependent on existing public databases, which may not be regularly updated with the latest information. Second, the anti-hyperpigmentation effect of THSWD was validated only at the *in vitro* level, lacking *in vivo* verification. Third, the therapeutic potential of THSWD in treating hyperpigmentation has not yet been clinically evaluated. To address these gaps, future efforts will focus on conducting *in vivo* studies to further substantiate the impact of THSWD on the ALB, IL6, and MAPK3 hub targets. Such studies will contribute to a stronger foundation for the development of targeted therapeutic interventions. Additionally, it is crucial to extend this research into clinical settings to assess the safety and efficacy of THSWD in diverse patient populations. This includes considering variables such as dosage, methods of administration, and long-term effects. Moreover, exploring the potential synergistic effects of the core compounds identified in THSWD, quercetin, apigenin, and luteolin, could lead to the optimization of the formula. By pursuing these research avenues, we aim to expand the scope of the current study, laying the groundwork for subsequent investigations and the clinical application of THSWD in the treatment of hyperpigmentation.

Conclusions

The present study used a combination of network pharmacology, molecular docking, and experimental verification to elucidate the mechanisms by which THSWD combats hyperpigmentation. Quercetin, apigenin, and luteolin are key compounds in THSWD, targeting ALB, IL6, and MAPK3. This research highlighted that the anti-hyperpigmentation effects of THSWD are primarily driven by anti-oxidative and anti-inflammatory responses. Additionally, the PI3K-Akt and MAPK signalling pathways are identified as being closely associated with THSWD's mechanisms against hyperpigmentation. This study shows the potential of THSWD as a treatment for hyperpigmentation, providing valuable information to researchers and clinicians in the quest for effective targeted therapies for this condition.

Author's contributions

The authors confirm contribution to the paper as follows: Conceptualization: JC; Data curation, Formal analysis, Investigation and Methodology: JC and WY; Project administration, Resources and Supervision: WY; Software: JC; Validation: WY; Visualization and Writing-original draft: JC; Writing-review & editing: WY. All authors reviewed the results and approved the final version of the manuscript.

Disclosure statement

No potential conflict of interest was reported by the author(s).

Funding

The author(s) reported there is no funding associated with the work featured in this article.

Data availability statement

The data that support the findings of this study are available from the corresponding author, [WY], upon reasonable request.

References

Ambrosio AL, Di Pietro SM. 2017. Storage pool diseases illuminate platelet dense granule biogenesis. Platelets. 28(2):138–146. doi: 10.1080/09537104.2016.1243789.

Bickerton GR, Paolini GV, Besnard J, Muresan S, Hopkins AL. 2012. Quantifying the chemical beauty of drugs. Nat Chem. 4(2):90–98. doi: 10.1038/nchem.1243.

Boo YC. 2019. p-Coumaric acid as an active ingredient in cosmetics: a review focusing on its antimelanogenic effects. Antioxidants (Basel). 8(8):275. doi: 10.3390/antiox8080275.

Burgess S, Thompson SG. 2017. Interpreting findings from Mendelian randomization using the MR-Egger method. Eur J Epidemiol. 32(5):377–389. doi: 10.1007/s10654-017-0255-x.

Carter AR, Sanderson E, Hammerton G, Richmond RC, Davey Smith G, Heron J, Taylor AE, Davies NM, Howe LD. 2021. Mendelian randomisation for mediation analysis: current methods and challenges for implementation. Eur J Epidemiol. 36(5):465–478. doi: 10.1007/s10654-021-00757-1.

Chae JK, Subedi L, Jeong M, Park YU, Kim CY, Kim H, Kim SY. 2017. Gomisin N Inhibits melanogenesis through regulating the PI3K/Akt and MAPK/ERK signaling pathways in melanocytes. Int J Mol Sci. 18(2):471. doi: 10.3390/ijms18020471.

Chaiprasongsuk A, Panich U. 2022. Role of phytochemicals in skin photoprotection via regulation of Nrf2. Front Pharmacol. 13:823881. doi: 10.3389/fphar.2022.823881.

Chang YH, Kim C, Jung M, Lim YH, Lee S, Kang S. 2007. Inhibition of melanogenesis by selina-4(14),7(11)-dien-8-one isolated from *Atractylodis* rhizoma Alba. Biol Pharm Bull. 30(4):719–723. doi: 10.1248/bpb.30.719.

Chen H, Boutros PC. 2011. VennDiagram: a package for the generation of highly-customizable Venn and Euler diagrams in R. BMC Bioinformatics. 12(1):35. doi: 10.1186/1471-2105-12-35.

Chen J, Chen H, Zhu Q, Liu Q, Zhou Y, Li L, Wang Y. 2022. Age at menarche and ischemic heart disease: an update mendelian randomization study. Front Genet. 13:942861. doi: 10.3389/fgene.2022.942861.

Chin CH, Chen SH, Wu HH, Ho CW, Ko MT, Lin CY. 2014. cytoHubba: identifying hub objects and sub-networks from complex interactome. BMC Syst Biol. 8 Suppl 4(Suppl 4):S11. doi: 10.1186/1752-0509-8-S4-S11.

Conway JR, Lex A, Gehlenborg N. 2017. UpSetR: an R package for the visualization of intersecting sets and their properties. Bioinformatics. 33(18):2938–2940. doi: 10.1093/bioinformatics/btx364.

Di Petrillo A, Orrù G, Fais A, Fantini MC. 2022. Quercetin and its derivates as antiviral potentials: a comprehensive review. Phytother Res. 36(1):266–278. doi: 10.1002/ptr.7309.

Ding XJ, Zhang ZY, Jin J, Han JX, Wang Y, Yang K, Yang YY, Wang HQ, Dai XT, Yao C, et al. 2020. Salidroside can target both P4HB-mediated inflammation and melanogenesis of the skin. Theranostics. 10(24):11110–11126.,. doi: 10.7150/thno.47413.

Dong D, Xu Z, Zhong W, Peng S. 2018. Parallelization of molecular docking: a review. Curr Top Med Chem. 18(12):1015–1028. doi: 10.2174/1568026618666180821145215.

Duran-Güell M, Flores-Costa R, Casulleras M, López-Vicario C, Titos E, Díaz A, Alcaraz-Quiles J, Horrillo R, Costa M, Fernández J, et al. 2021. Albumin protects the liver from tumor necrosis factor α-induced immunopathology. Faseb J. 35(2):e21365. doi: 10.1096/fj.202001615RRR.

Feng C, Zhao M, Jiang L, Hu Z, Fan X. 2021. Mechanism of modified Danggui Sini decoction for knee osteoarthritis based on network pharmacology and molecular docking. Evid Based Complement Alternat Med. 2021:6680637–6680611. doi: 10.1155/2021/6680637.

Fu C, Chen J, Lu J, Yi L, Tong X, Kang L, Pei S, Ouyang Y, Jiang L, Ding Y, et al. 2020. Roles of inflammation factors in melanogenesis (Review). Mol Med Rep. 21:1421–1430.

Gendrisch F, Esser PR, Schempp CM, Wölfle U. 2021. Luteolin as a modulator of skin aging and inflammation. Biofactors. 47(2):170–180. doi: 10.1002/biof.1699.

Giménez García RM, Carrasco Molina S. 2019. Drug-induced hyperpigmentation: review and case series. J Am Board Fam Med. 32(4):628–638. doi: 10.3122/jabfm.2019.04.180212.

Goodsell DS, Zardecki C, Di Costanzo L, Duarte JM, Hudson BP, Persikova I, Segura J, Shao C, Voigt M, Westbrook JD, et al. 2020. RCSB Protein Data Bank: enabling biomedical research and drug discovery. Protein Sci. 29(1):52–65.,. doi: 10.1002/pro.3730.

Guo H, Zeng H, Fu C, Huang J, Lu J, Hu Y, Zhou Y, Luo L, Zhang Y, Zhang L, et al. 2021. Identification of sitogluside as a potential skin-pigmentation-reducing agent through network pharmacology. Oxid Med Cell Longev. 2021:4883398–4883316. doi: 10.1155/2021/4883398.

Honisch C, Gazziero M, Dallocchio R, Dessì A, Fabbri D, Dettori MA, Delogu G, Ruzza P. 2022. Antamanide analogs as potential inhibitors of tyrosinase. Int J Mol Sci. 23(11):6240. doi: 10.3390/ijms23116240.

Huang L, Xie D, Yu Y, Liu H, Shi Y, Shi T, Wen C. 2018. TCMID 2.0: a comprehensive resource for TCM. Nucleic Acids Res. 46:1117–1120.

Huang S, Chen Y, Pan L, Fei C, Wang N, Chu F, Peng D, Duan X, Wang Y. 2021. Exploration of the potential mechanism of Tao Hong Si Wu decoction for the treatment of breast cancer based on network pharmacology and *in vitro* rxperimental verification. Front Oncol. 11:731522. doi: 10.3389/fonc.2021.731522.

Huang XF, Zhang JL, Huang DP, Huang AS, Huang HT, Liu Q, Liu XH, Liao HL. 2020. A network pharmacology strategy to investigate the anti-inflammatory mechanism of luteolin combined with in vitro transcriptomics and proteomics. Int Immunopharmacol. 86:106727. doi: 10.1016/j.intimp.2020.106727.

Hwang E, Lee TH, Lee WJ, Shim WS, Yeo EJ, Kim S, Kim SY. 2016. A novel synthetic *Piper* amide derivative NED-180 inhibits hyperpigmentation by activating the PI3K and ERK pathways and by regulating Ca2+ influx via TRPM1 channels. Pigment Cell Melanoma Res. 29(1):81–91. doi: 10.1111/pcmr.12430.

Imran M, Rauf A, Abu-Izneid T, Nadeem M, Shariati MA, Khan IA, Imran A, Orhan IE, Rizwan M, Atif M, et al. 2019. Luteolin, a flavonoid, as an anticancer agent: a review. Biomed Pharmacother. 112:108612.,. doi: 10.1016/j.biopha.2019.108612.

Jiang H, Li M, Du K, Ma C, Cheng Y, Wang S, Nie X, Fu C, He Y. 2021. Traditional Chinese medicine for adjuvant treatment of breast cancer: taohong Siwu Decoction. Chin Med. 16(1):129. doi: 10.1186/s13020-021-00539-7.

Karadeniz F, Oh JH, Seo Y, Yang J, Lee H, Kong CS. 2023. Quercetin 3-O-galactoside isolated from *Limonium tetragonum* inhibits melanogenesis by regulating PKA/MITF signaling and ERK activation. Int J Mol Sci. 24(4):3064. doi: 10.3390/ijms24043064.

Khasawneh LQ, Al-Mahayri ZN, Ali BR. 2022. Mendelian randomization in pharmacogenomics: the unforeseen potentials. Biomed Pharmacother. 150:112952. doi: 10.1016/j.biopha.2022.112952.

Kim S, Chen J, Cheng T, Gindulyte A, He J, He S, Li Q, Shoemaker BA, Thiessen PA, Yu B, et al. 2021. PubChem in 2021: new data content and improved web interfaces. Nucleic Acids Res. 49:1388–1395.

Kumar K, Chupakhin V, Vos A, Morrison D, Rassokhin D, Dellwo MJ, McCormick K, Paternoster E, Ceulemans H, DesJarlais RL. 2021. Development and implementation of an enterprise-wide predictive model for early absorption, distribution, metabolism and excretion properties. Future Med Chem. 13(19):1639–1654. doi: 10.4155/fmc-2021-0138.

Kumari S, Tien Guan Thng S, Kumar Verma N, Gautam HK. 2018. Melanogenesis inhibitors. Acta Derm Venereol. 98(10):924–931. doi: 10.2340/00015555-3002.

Lee SE, Park SH, Oh SW, Yoo JA, Kwon K, Park SJ, Kim J, Lee HS, Cho JY, Lee J. 2018. Beauvericin inhibits melanogenesis by regulating cAMP/PKA/CREB and LXR-α/p38 MAPK-mediated pathways. Sci Rep. 8(1):14958. doi: 10.1038/s41598-018-33352-8.

Legeay M, Doncheva NT, Morris JH, Jensen LJ. 2020. Visualize omics data on networks with Omics Visualizer, a Cytoscape App. F1000Res. 9:157. doi: 10.12688/f1000research.22280.2.

Li J, Jiang S, Huang C, Yang X. 2022. Atraric acid ameliorates hyperpigmentation through the downregulation of the PKA/CREB/MITF signaling pathway. Int J Mol Sci. 23(24):15952. doi: 10.3390/ijms232415952.

Li M, Xiao YB, Wei L, Liu Q, Liu PY, Yao JF. 2022. Beneficial effects of traditional Chinese medicine in the treatment of premature ovarian failure. Evid Based Complement Alternat Med. 2022:5413504. doi: 10.1155/2022/5413504.

Li X, Chen H, Yang H, Liu J, Li Y, Dang Y, Wang J, Wang L, Li J, Nie G. 2022. Study on the potential mechanism of tonifying kidney and removing dampness formula in the treatment of postmenopausal dyslipidemia based on network pharmacology, molecular docking and experimental evidence. Front Endocrinol (Lausanne). 13:918469. doi: 10.3389/fendo.2022.918469.

Liu J, Jiang R, Zhou J, Xu X, Sun Z, Li J, Chen X, Li Z, Yan X, Zhao D, et al. 2021. Salicylic acid in ginseng root alleviates skin hyperpigmentation disorders by inhibiting melanogenesis and melanosome transport. Eur J Pharmacol. 910:174458. doi: 10.1016/j.ejphar.2021.174458.

Liu P, Wang W, Li Z, Li Y, Yu X, Tu J, Zhang Z, Czuczejko J. 2022. Ferroptosis: a new regulatory mechanism in osteoporosis. Oxid Med Cell Longev. 2022:2634431. doi: 10.1155/2022/2634431.

Liu X, Rao J, Wang K, Wang M, Yao T, Qiu F. 2022. Highly potent inhibition of tyrosinase by mulberrosides and the inhibitory mechanism *in vitro*. Chem Biodivers. 19:e202100740.

Lu H, Wu PF, Zhang W, Liao X. 2021. Circulating interleukins and risk of multiple sclerosis: a mendelian randomization study. Front Immunol. 12:647588. doi: 10.3389/fimmu.2021.647588.

Lu Y, Tonissen KF, Di Trapani G. 2021. Modulating skin colour: role of the thioredoxin and glutathione systems in regulating melanogenesis. Biosci Rep. 41(5): BSR20210427. doi: 10.1042/BSR20210427.

Lu Y, Xu Y, Song MT, Qian LL, Liu XL, Gao RY, Han RM, Skibsted LH, Zhang JP. 2021. Promotion effects of flavonoids on browning induced by enzymatic oxidation of tyrosinase: structure-activity relationship. RSC Adv. 11(23):13769–13779. doi: 10.1039/d1ra01369f.

Luo L, Yu X, Zeng H, Hu Y, Jiang L, Huang J, Fu C, Chen J, Zeng Q. 2023. Fraxin inhibits melanogenesis by suppressing the ERK/MAPK pathway and antagonizes oxidative stress by activating the NRF2 pathway. Heliyon. 9(8):e18929. doi: 10.1016/j.heliyon.2023.e18929.

Lussi YC, Magrane M, Martin MJ, Orchard S, UniProt C. 2023. Searching and Navigating UniProt Databases. Curr Protoc. 3:e700.

Lyon MS, Andrews SJ, Elsworth B, Gaunt TR, Hemani G, Marcora E. 2021. The variant call format provides efficient and robust storage of GWAS summary statistics. Genome Biol. 22(1):32. doi: 10.1186/s13059-020-02248-0.

Ma X, Shao S, Xiao F, Zhang H, Zhang R, Wang M, Li G, Yan M. 2021. *Platycodon grandiflorum* extract: chemical composition and whitening, antioxidant, and anti-inflammatory effects. RSC Adv. 11(18):10814–10826. doi: 10.1039/d0ra09443a.

Ma Z, Xu J, Ru L, Zhu W. 2021. Identification of pivotal genes associated with the prognosis of gastric carcinoma through integrated analysis. Biosci Rep. 41: BSR20203676.

Mann T, Gerwat W, Batzer J, Eggers K, Scherner C, Wenck H, Stäb F, Hearing VJ, Röhm K-H, Kolbe L. 2018. Inhibition of human tyrosinase requires molecular Motifs distinctively different from mushroom tyrosinase. J Invest Dermatol. 138(7):1601–1608. doi: 10.1016/j.jid.2018.01.019.

Mattos KPH, Cintra ML, Gouvêa IR, Ferreira L, Velho P, Moriel P. 2017. Skin hyperpigmentation following intravenous polymyxin B treatment associated with melanocyte activation and inflammatory process. J Clin Pharm Ther. 42(5):573–578. doi: 10.1111/jcpt.12543.

Menasche BL, Crisman L, Gulbranson DR, Davis EM, Yu H, Shen J. 2019. Fluorescence activated cell sorting (FACS) in genome-wide genetic screening of membrane trafficking. Curr Protoc Cell Biol. 82(1):e68. doi: 10.1002/cpcb.68.

Nautiyal A, Wairkar S. 2021. Management of hyperpigmentation: current treatments and emerging therapies. Pigment Cell Melanoma Res. 34(6): 1000–1014. doi: 10.1111/pcmr.12986.

Nishina A, Miura A, Goto M, Terakado K, Sato D, Kimura H, Hirai Y, Sato H, Phay N. 2018. Mansonone E from *Mansonia gagei* inhibited α-MSH-induced melanogenesis in B16 cells by inhibiting CREB expression and phosphorylation in the PI3K/Akt pathway. Biol Pharm Bull. 41(5):770–776. doi: 10.1248/bpb.b17-01045.

Pan L, Peng C, Wang L, Li L, Huang S, Fei C, Wang N, Chu F, Peng D, Duan X. 2022. Network pharmacology and experimental validation-based approach to understand the effect and mechanism of Taohong Siwu Decoction

against ischemic stroke. J Ethnopharmacol. 294:115339. doi: 10.1016/j.jep.2022.115339.
Pinero J, Ramirez-Anguita JM, Sauch-Pitarch J, Ronzano F, Centeno E, Sanz F, Furlong LI. 2020. The DisGeNET knowledge platform for disease genomics: 2019 update. Nucleic Acids Res. 48:845–855.
Pinzi L, Rastelli G. 2019. Molecular docking: shifting paradigms in drug discovery. Int J Mol Sci. 20(18):4331. doi: 10.3390/ijms20184331.
Plensdorf S, Livieratos M, Dada N. 2017. Pigmentation disorders: diagnosis and management. Am Fam Physician. 96(12):797–804.
Ru J, Li P, Wang J, Zhou W, Li B, Huang C, Li P, Guo Z, Tao W, Yang Y, et al. 2014. TCMSP: a database of systems pharmacology for drug discovery from herbal medicines. J Cheminform. 6:13.,. doi: 10.1186/1758-2946-6-13.
Safran M, Dalah I, Alexander J, Rosen N, Iny Stein T, Shmoish M, Nativ N, Bahir I, Doniger T, Krug H, et al. 2010. GeneCards Version 3: the human gene integrator. Database (Oxford). 2010:baq020. doi: 10.1093/database/baq020.
Seeliger D, de Groot BL. 2010. Ligand docking and binding site analysis with PyMOL and Autodock/Vina. J Comput Aided Mol Des. 24(5):417–422. doi: 10.1007/s10822-010-9352-6.
Shao CL, Cui GH, Guo HD. 2022. Effects and mechanisms of Taohong Siwu decoction on the prevention and treatment of myocardial injury. Front Pharmacol. 13:816347. doi: 10.3389/fphar.2022.816347.
Shi Y, Cai J, Shi C, Liu C, Zhou J, Li Z. 2022. Low serum albumin is associated with poor prognosis in patients receiving peritoneal dialysis treatment. J Healthc Eng. 2022:7660806. doi: 10.1155/2022/7660806.
Shi Y, Liu Q, Chen W, Wang R, Wang L, Liu ZQ, Duan XC, Zhang Y, Shen A, Peng D, et al. 2023. Protection of Taohong Siwu decoction on PC12 cells injured by oxygen glucose deprivation/reperfusion via mitophagy-NLRP3 inflammasome pathway *in vitro*. J Ethnopharmacol. 301:115784. doi: 10.1016/j.jep.2022.115784.
Sun L, Guo C, Yan L, Li H, Sun J, Huo X, Xie X, Hu J. 2020. Syntenin regulates melanogenesis via the p38 MAPK pathway. Mol Med Rep. 22(2):733–738. doi: 10.3892/mmr.2020.11139.
Sun L, Guo Y, Zhang Y, Zhuang Y. 2017. Antioxidant and anti-tyrosinase activities of phenolic extracts from rape bee [pollen and inhibitory melanogenesis by cAMP/MITF/TYR pathway in B16 mouse melanoma cells. Front Pharmacol. 8:104. doi: 10.3389/fphar.2017.00104.
Szklarczyk D, Gable AL, Nastou KC, Lyon D, Kirsch R, Pyysalo S, Doncheva NT, Legeay M, Fang T, Bork P, et al. 2021. The STRING database in 2021: customizable protein-protein networks, and functional characterization of user-uploaded gene/measurement sets. Nucleic Acids Res. 49:605–612.
Tang Z, Yin M, Guo Y, Li W, Sun F, Guo Y, Chen Z, Zhou B. 2022. Taohong Siwu decoction promotes osteo-angiogenesis in fractures by regulating the HIF-1α signaling pathway. Evid Based Complement Alternat Med. 2022:6777447–6777410. doi: 10.1155/2022/6777447.
Wang N, Fei C, Chu F, Huang S, Pan L, Peng D, Duan X. 2021. Taohong Siwu decoction regulates cell necrosis and neuroinflammation in the rat middle cerebral artery occlusion model. Front Pharmacol. 12:732358. doi: 10.3389/fphar.2021.732358.
Wenner K, Ramberg T. 2022. An open-label study assessing the efficacy and tolerability of a skincare regimen in subjects of different ethnicities with moderate-to-severe hyperpigmentation. J Cosmet Dermatol. 21(6):2497–2507. doi: 10.1111/jocd.14447.
Wu Q, Li W, Zhao J, Sun W, Yang Q, Chen C, Xia P, Zhu J, Zhou Y, Huang G, et al. 2021. Apigenin ameliorates doxorubicin-induced renal injury via inhibition of oxidative stress and inflammation. Biomed Pharmacother. 137:111308. doi: 10.1016/j.biopha.2021.111308.
Xia W, Hu S, Wang M, Xu F, Han L, Peng D. 2021. Exploration of the potential mechanism of the Tao Hong Si Wu Decoction for the treatment of postpartum blood stasis based on network pharmacology and *in vivo* experimental verification. J Ethnopharmacol. 268:113641. doi: 10.1016/j.jep.2020.113641.
Xing X, Dan Y, Xu Z, Xiang L. 2022. Implications of oxidative stress in the pathogenesis and treatment of hyperpigmentation disorders. Oxid Med Cell Longev. 2022:7881717–7881712. doi: 10.1155/2022/7881717.
Xu Z, Chen L, Jiang M, Wang Q, Zhang C, Xiang LF. 2018. CCN1/Cyr61 Stimulates melanogenesis through integrin α6β1, p38 MAPK, and ERK1/2 signaling pathways in human epidermal melanocytes. J Invest Dermatol. 138(8):1825–1833. doi: 10.1016/j.jid.2018.02.029.
Yan D, Zheng G, Wang C, Chen Z, Mao T, Gao J, Yan Y, Chen X, Ji X, Yu J, et al. 2022. HIT 2.0: an enhanced platform for herbal ingredients' targets. Nucleic Acids Res. 50:1238–1243.
Yan X, Ma X, Dai D, Yan X, Han X, Bao X, Xie Q. 2023. Potent pigmentation inhibitory activity of incensole-enriched frankincense volatile oil-identification, efficacy and mechanism. J Cosmet Dermatol. 23(1):244–255. doi: 10.1111/jocd.15887.
Yang M, Chen J, Xu L, Shi X, Zhou X, An R, Wang X. 2018. A network pharmacology approach to uncover the molecular mechanisms of herbal formula Ban-Xia-Xie-Xin-Tang. Evid Based Complement Alternat Med. 2018:4050714–4050722. doi: 10.1155/2018/4050714.
Yang MQ, Chen C, Mao YF, Li Y, Zhong X, Yu YD, Xue YT, Song YM. 2022. Application of network pharmacology and molecular docking approach to explore active compounds and potential pharmacological mechanisms of Aconiti Lateralis Radix Praeparata and Lepidii Semen Descurainiae Semen for treatment of heart failure. Medicine (Baltimore). 101(33):e30102. doi: 10.1097/MD.0000000000030102.
Yoo J. 2022. Differential diagnosis and management of hyperpigmentation. Clin Exp Dermatol. 47(2):251–258. doi: 10.1111/ced.14747.
Yu G, Wang LG, Han Y, He QY. 2012. clusterProfiler: an R package for comparing biological themes among gene clusters. OMICS. 16(5):284–287. doi: 10.1089/omi.2011.0118.
Yun CY, You ST, Kim JH, Chung JH, Han SB, Shin EY, Kim EG. 2015. p21-activated kinase 4 critically regulates melanogenesis via activation of the CREB/MITF and β-catenin/MITF pathways. J Invest Dermatol. 135(5):1385–1394. doi: 10.1038/jid.2014.548.
Zhang Z, He S, Yu Q, Ding J. 2023. Clinical study of modified photodynamic therapy combined with Taohong Siwu Decoction in treating hypertrophic scar after severe burn. Clinics (Sao Paulo). 78:100295. doi: 10.1016/j.clinsp.2023.100295.
Zhao J, Dan Y, Liu Z, Wang Q, Jiang M, Zhang C, Sheu HM, Lin CS, Xiang L. 2022. Solamargine alleviated UVB-induced inflammation and melanogenesis in human keratinocytes and melanocytes via the p38 MAPK signaling pathway, a promising agent for post-inflammatory hyperpigmentation. Front Med (Lausanne). 9:812653. doi: 10.3389/fmed.2022.812653.
Zhou J, Yang D, Zhou SH, Wang JP, Liu YS, Wang SL. 2018. Clinical efficacy and safety of bathing with Chinese medicine Taohong Siwu decoction for treatment of diffuse cutaneous systemic sclerosis: a randomized placebo-controlled trial. Chin J Integr Med. 24(3):185–192. doi: 10.1007/s11655-017-2954-2.
Zhou S, Sakamoto K. 2019. Pyruvic acid/ethyl pyruvate inhibits melanogenesis in B16F10 melanoma cells through PI3K/AKT, GSK3β, and ROS-ERK signaling pathways. Genes Cells. 24(1):60–69. doi: 10.1111/gtc.12654.
Zhou S, Sakamoto K. 2020. Citric acid promoted melanin synthesis in B16F10 mouse melanoma cells, but inhibited it in human epidermal melanocytes and HMV-II melanoma cells via the GSK3β/β-catenin signaling pathway. PLoS One. 15(12):e0243565. doi: 10.1371/journal.pone.0243565.
Zhu W, Li Y, Zhao J, Wang Y, Li Y, Wang Y. 2022. The mechanism of triptolide in the treatment of connective tissue disease-related interstitial lung disease based on network pharmacology and molecular docking. Ann Med. 54(1):541–552. doi: 10.1080/07853890.2022.2034931.